Hyperspectral Imaging for Readability Enhancement of Historic Manuscripts

- revised version, August 2018 -

Simon Mindermann

simon.mindermann@tum.de

Thesis submitted in partial fulfillment of the requirements for the degree

Master of Arts (M.A.)

Chair for Conservation-Restoration,
Art Technology and Conservation Science

Faculty of Architecture

Technical University of Munich

In cooperation with the

Institute for Restoration and Conservation

Bavarian State Library Munich

Date of Submission:	31.01.2018, Munich
1st supervisor:	Dr. Thorsten Allscher
2nd supervisor:	Prof. Erwin Emmerling

Declaration of Authorship

I hereby declare that I have written this master's thesis independently and have used no other than the specified tools. All passages taken from the text or meaning of other sources are identified by reference according to the usual rules of scientific citation (including the World Wide Web and other electronic text and databases). This also applies to drawings, pictorial representations, sketches, tables and the like. I am aware that false statements are treated as an attempt to deceive and that in case of suspicion, all methods of plagiarism detection can be applied.

This paper was not previously presented to another examination board and has not been published.

Simon Mindermann, Munich, January the 31st 2018.

Acknowledgement

I would like to thank Dr. Thorsten Allscher and Dr. Irmhild Ceynowa of the Bavarian State Library for giving me the opportunity to carry out this work and use the hyperspectral imaging system of the Bavarian State Library. I further express my thanks to Prof. Erwin Emmerling and all members of the Chair of Conservation-Restoration, Art Technology and Conservation Science of the Technical University of Munich.

Mein besonderer Dank gilt Diana, Helena und Benjamin!

Abstract

Hyperspectral Imaging (HSI) is considered a capable tool for the analysis of faded or deliberately erased historic documents. In HSI, the spectral reflectance properties of the documents are registered with high precision across the visible light (VIS) and near infrared (NIR) regions of the electromagnetic spectrum (EMS). The resulting data set contains the photographic (spatial) information combined with the spectral information for each pixel. Varying reflectance intensities of different materials can allow for an increased contrast of paper/parchment and ink. By using supervised and unsupervised multivariate image processing techniques, the visibility of the text can be enhanced or restored making use of the data's statistics. Most of the techniques used are derived from the field of remote sensing. To validate the effectiveness of several techniques proposed in the literature, their exemplary application to different historic manuscripts is presented in this work. To enhance the spectral and spatial quality of the scans, pre-processing steps like noise reduction and spectral sharpening are employed. Then, unsupervised transformation methods (principal component analysis – PCA, independent component analysis – ICA and minimum noise fraction transformation – MNF) are applied to different analytical tasks and their potential usefulness in legibility enhancement is confirmed. Supervised classification methods (spectral angle mapping – SAM and mahalanobis distance classification – MahDC) showed to deliver high quality classification images, if the scriptures are well enough separable.

In this work, the high versatility of HSI for legibility enhancement of historic manuscripts was confirmed. The technique provides a toolset for various issues and can be adapted to the diverse objects that are expected in this field of application, like the separation of different, overlaying scriptures or the attenuation of disturbing background effects. In the process of digitization, cultural institutions like museums and libraries are increasingly focusing on the online presentation of their collections and research. HSI can provide highly informative images that allow for a direct communication of scientific findings to scientists, working with the historic texts, as well as to a large general online audience.

Zusammenfassung

Hyperspectral Imaging (HSI) ist eine mögliche Methode zur Sichtbarmachung verblichener oder gelöschter Texte von historischen Dokumenten. Die Reflexionseigenschaften der Schriftstücke im Bereich des sichtbaren Lichts (VIS) und des angrenzenden Infrarotbereichs (NIR) des elektromagnetischen Spektrums (EMS) werden mit hoher spektraler Auflösung gescannt. Der gewonnene Datensatz beinhaltet die photographische Information, ebenso wie die spektrale Information für jeden Bildpixel. Die multivariate Bildverarbeitung arbeitet mit mathematischen, statistischen und stochastischen Methoden, um den Datensatz zu analysieren und transformieren, um eine bessere Lesbarkeit der gesuchten Texte zu erhalten. In der vorliegenden Arbeit werden in der Literatur vorgeschlagene Methoden an verschiedenen historischen Schriftstücken erprobt. Um ideale Bedingungen für die anschließende Analyse zu erhalten, werden zunächst verschiedene Vorverarbeitungsschritte (Reduktion von Bildrauschen, erhöhen der lokalen Bildschärfe) ausgeführt. Danach werden unüberwachte Bildtransformationstechniken (Hauptkomponentenanalyse - PCA, unabhängige Komponentenanalyse - ICA, Minimum Noise Fraction Transformation - MNF) an unterschiedlichen Beispielen zur Verbesserung der Lesbarkeit eingesetzt. Methoden der überwachten Bildklassifizierung werden ebenfalls erprobt, um eindeutige Kartierungen der vorhandenen Tinten zu erzeugen. Es zeigte sich, dass insbesondere die unüberwachten Techniken sehr gute Ergebnisse liefern können, wenn die verschiedenen Tinten und Materialien eine ausreichende spektrale Differenzierbarkeit aufweisen. Insbesondere die Kartierung mit überwachten Klassifizierungsalgorithmen eignet sich, um ansprechende und informative Bilder zu erzeugen, die sich für die Präsentation der Forschungsergebnisse, beispielsweise im Internet eignen.

Contents

1 List of Important Abbreviations

ACE	adaptive coherence estimator
BSB	Bayerische Staatsbibliothek München - Bavarian State Library
BSS	blind source separation
CCD	charge-coupled device
CEM	constrained energy minimization
DNB	Deutsche Nationalbibliothek Bamberg - German National Library of Bamberg
EMS	electromagnetic spectrum
FFT	fast fourier transform
HSI	hyperspectral imaging
IBR	Institut für Bestandserhaltung und Restaurierung - Institute for Conservation and Restoration of the Bavarian State Library
ICA	independent component analysis
IC	independent component
LED	light-emitting diode
MaDC	mahalanobis distance classification
MF	matched filter
MinDC	minimum distance classification
MLC	maximum likelihood classification
MNF	minimum noise fraction transformation
MSI	multispectral imaging
NIR	near infrared
OCR	optical character recognition
Pan	panchromatic image
PCA	principal component analysis
PC	principal component
ROI	region of interest
SAM	spectral angle mapping
SMACC	sequential maximum angle convex cone
SWIR	short-wave infrared
UV	ultraviolet
VIS	visible light
VNIR	visible light and near infrared

2 Introduction

2.1 Digital Imaging in Cultural Heritage Science

In the field of cultural heritage science, working mostly with visually perceivable objects, images play a vital role in the accumulation, as well as the communication of scientific findings. Scientific image analysis and processing now provide the chance, to communicate scientific results in their most intuitively comprehensible form: As images. The human ability to quickly grasp visual content, combined with the capability of modern imaging systems to generate images containing a vast amount of information, has resulted in a number of recent publications with extensive public perception, ranging from the visualization of formerly unreadable treatises of Archimedes[1], hidden paintings by Van Gogh[2] or Degas[3], to the finding of unknown “rooms” in the Great Pyramid (Khufu’s Pyramid)[4].

Although exploiting radiation from extremely different regions of the electromagnetic spectrum (EMS) and investigating on objects with enormously different dimensions, all these undertakings follow closely related goals: To identify, extract and visualize features of the objects, that are not apparent under normal lighting conditions. To further the knowledge about the materials and production techniques and shed light on the history of material cultural heritage, or to aid in authorship and provenance questions, as well as conservatory investigations on deterioration, hidden defects or damage assessment, are only some of the possible applications

The digitization, being one of the major technological developments in the 21st century, makes it possible to provide vast amounts of imagery to scientists, but also the broad online community. Technology companies like Google have recently started their own digitization-platforms, solely for cultural heritage objects and there are many different expectations and promises surrounding these new developments.[5] The rapidly growing online-databases of digitized artworks make digital copies in very high quality available, to every person with access to the internet. With 3d-printing technology still evolving, physical copies, based on the digitized artworks, could become broadly available as well, in the near future. Ultimately, the digitization is seen as a means against accelerated deterioration by presentation and visitor access and a method to save copies of works of art, endangered by vandalism or deliberate destruction.

[1] EASTON/NOEL (2010).
[2] DIK ET AL. (2008).
[3] THURROWGOOD ET AL. (2016).
[4] MORISHIMA ET AL. (2017).
[5] Google Cultural Institute: https://www.google.com/culturalinstitute/beta/

In all this, the production and processing of digital images with meaningful scientific content is an essential task for cultural heritage scientists. The analysis of imagery has always been a major part in any scientific approach to art. Thus the extension to digital imaging, exploiting wide regions of the EMS, and the above mentioned benefits of image processing is a logical step to take. The analysis of manuscripts, with the goal to enhance illegible or obscured writings, has been one major driving force behind this development.

2.2 Manuscript Analysis

The scientific analysis of historic manuscripts using imaging techniques has a long-ranging history. EASTON ET AL. (2014) summarize this history and report early attempts to use photographic techniques, to enhance the readability of historic manuscripts, to date into the mid-1890s.[6] The basic idea behind these experiments, remained paradigmatic for most imaging enterprises, for almost 100 years: To try to gain a better legibility of obscured, erased, faded or damaged writings by exposing the manuscript to radiation of different energies, and measure its characteristic interaction. A major impact on the development of new methods in this field, was made by the famous rediscovery of the oldest known copy of seven treatises by Archimedes in a medieval prayer book. The original codex was disassembled in the 10th, and again in the 13th century and the text erased, to be rewritten with a newer text. Such a manuscript is called a palimpsest, in which an older text was removed, chemically or physically, and which was then re-written with one or more younger writings. This was common practice in pre-modern times, regarding the high cost of parchment as writing material. The manuscript pages were often turned, cut and re-arranged and ultimately bound in a new book. A lot of old writings are also regularly found as maculatory paper in the bindings of medieval codices, which was another way of recycling no longer needed books.

The imaging of the Achimedes Palimpsest between 2000 and 2011 led not only to great public interest in the possibilities of spectral imaging applied to historic manuscripts, but also to the adaption and development of a variety of methods for the purpose of legibility enhancement. It was one of the first uses of sophisticated multispectral imaging in the ultraviolet (UV: approximately 100 to 400 nm), visible (VIS: approximately 400 to 700 nm) and near-infrared (NIR: approximately 700 to 1400 nm) ranges of the EMS, along with a specially developed workflow for image processing. Later, synchrotron X-ray fluorescence imaging and improved multispectral imaging with modified illumination systems were integrated.[7]

[6] EASTON ET AL. (2014), p. 36.
[7] EASTON ET AL. (2014), pp. 67-70.

2.3 Scope of this Work

In this thesis a practical approach to the problem of readability enhancement of ancient manuscripts using spectral imaging techniques is presented. Chapter 3 introduces the basic concepts of spectral imaging and digital multivariate image processing. The reader is familiarized with important concepts and algorithms, most of which will be applied in chapter 4 for the analysis of different manuscripts. Hyperspectral imaging and multivariate image analysis were used in these applications, to show possible solutions to the presented, re-occurring issues of readability enhancement. The topics in focus are the imaging of obscured writings, the reduction of recto-verso bleed-through or see-through, and the legibility enhancement of palimpsests. Three historic documents from the BSB (shelfmarks: Clm 29416, Clm 29418 and St.th. 957) and one from the Deutsche Nationalbibliothek Bamberg (DNB) (Msc.patr. 5) were used, all of which are currently being topics of active research.

3 Spectral Imaging

3.1 Multivariate Digital Imagery

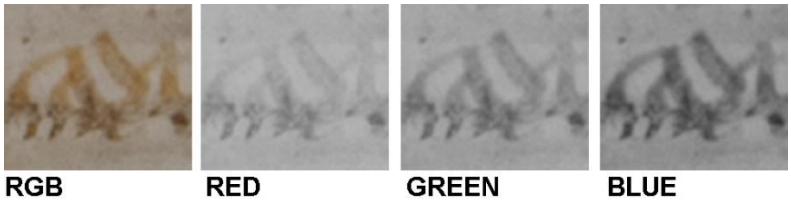

Figure 1: Digital RGB-photograph. Detail of Clm 29416 1-verso. Left to right: RGB-color image and split up into red, green and blue channels as greyscale images

A digital greyscale image can be described as a two-dimensional array of intensity values (between 0=black … 255=white, in a conventional 8-bit image) with I columns and J rows, or an $I * J$ matrix. A conventional digital color image expands the grayscale dimension to three color intensity values, usually red green and blue, thus becoming a multivariate image, that bears more than one feature per observation (figure 1). The information of these color channels together describes any color that can be reproduced within the respective color-space. Thus, a multivariate image is characterized by an $I * J * K$ matrix with K being referred to as the image variables. Another important concept is the vector form of any individual image pixel, as an N-dimensional vector with N equaling the number of spectral bands and the values of $x_1 \cdots x_N$ given by the registered reflectance values in the discrete bands.

$$x = \begin{bmatrix} x_1 \\ x_2 \\ \cdots \\ x_N \end{bmatrix}$$

Being readily describable in mathematical terms, digital images can be modified, transformed and analyzed by mathematical operations.[8] [9]

There can be more than three variables if the spectral range is split into more narrow channels, or spectral information from regions beyond the visible light are added (figure 2). The idea behind spectral imaging lies in the exploitation of such additional information. This information can be used exploratively, for example, a photograph taken under ultraviolet-radiation that enhances the contrast between faded writings and the strongly fluorescing parchment. The reflection of surfaces under certain lighting conditions is an important observation that can also be used to describe chemical and physical properties. Pixels showing the same spectral response in distinct bands, are likely to be physically related as well. By adding more observations (spectral bands) for each pixel, the materials can be described with additional variables and, theoretically, added precision. On the downside, the amount of data increases rapidly with every added band, spreading the information in a vast, multidimensional matrix. Thus, a statistical approach, that tries to find relationships within the “data-table” (being the digital image) to identify clusters of statistically connected pixel-vectors, could add to the knowledge of present materials in a more indirect way.

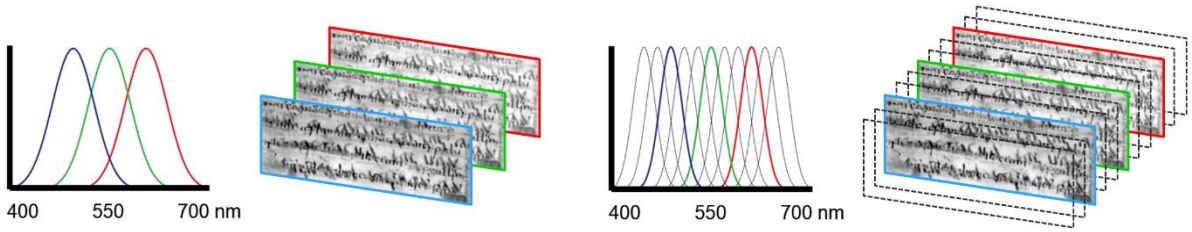

Figure 2: Approximate spectral bandwidths of a digital photograph (left) and a multispectral image (right). Schematic illustration

To the human perceptive system, information presented in a visual way is much easier to process than in any other form. Image analysis is therefore not only used to extract, but also to visualize information. By combining, filtering and transforming the input image-matrix, new images are created that aim to distill all relevant spectral, spatial and statistical information into a few, concentrated and highly informative greyscale images.

Technically, the number of spectral bands is limited mostly by the technology of the recording system and advanced strongly within the recent decades. The most important driving force behind this is the field of remote sensing. In the 1980s, the terms multispectral and hyperspectral imaging (MSI, HSI) were shaped to characterize multi-band spectroscopic

[8] GELADI/GRAHN (2007), p 1-5.
[9] RICHARDS/JIA (2006), p. 77.

images of the earth, taken from satellite and aircraft-carried scanners. These systems measure the earth's surface reflection for a variety of geological, biological, engineering and other applications. The discrimination between HSI and MSI is not strictly defined and differs between applications. MSIs are usually built of less than 100 spectral bands. An HSI comprises hundreds or thousands of bands in a much wider part of the EMS with a spectral resolution an order of magnitude higher. Also, MSI bands are usually of broader and more irregular width. [10] The term spectral imaging encompasses both, MSI and HSI.

Multiband image datasets are often depicted as image-cubes, three-dimensional representations of the data with the spatial coordinates X and Y and the spectral coordinate on the Z-axis (figure 3).

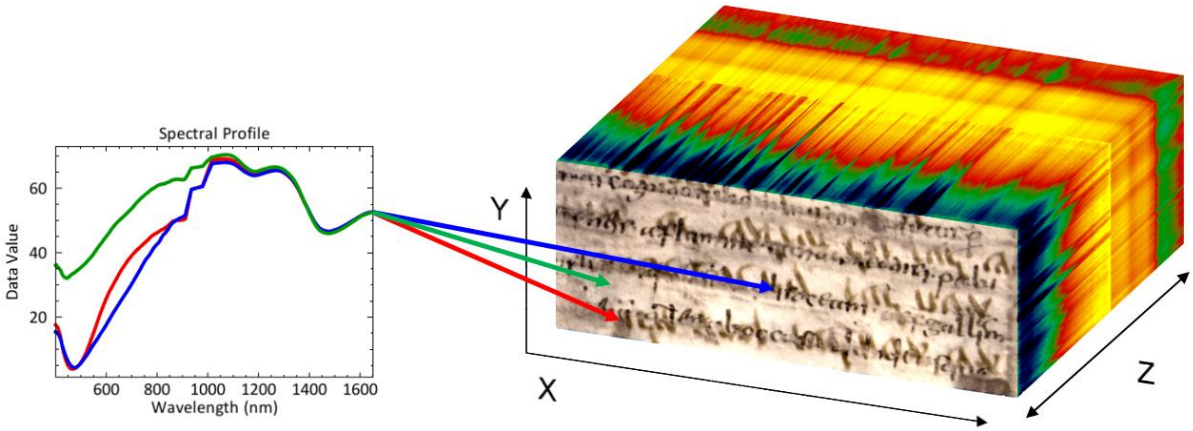

Figure 3: Illustration of a hyperspectral image cube (right) with different Z-axis point-profiles (left)

The high spectral resolution of HSI allows to plot the spectral information of each pixel as a reflectance spectrum (Z-axis profile) identical to a point spectrum obtained through a spectroscopic measurement (e. g. UV-VIS spectrometry). Slicing the cube in X-Y planes yields intensity mappings of a spectral band that are displayed as greyscale images, but any other geometric sampling is possible as well, resulting in different intensity profiles.

The spatial resolution is a second important category for spectral imaging systems. It is defined as the ability to separate the intensity value of two neighboring points in an image. Any spectral imaging system shows a compromise between these two factors since a high spectral and spatial resolution at the same time would inflate the technological and economical expenses.

[10] Spectral resolution (KEREKES/SCHOTT (2007), p. 19.): Central wavelength divided by width of the spectral band $\lambda/\Delta\lambda$;

While it is possible to increase the resolutions in the image processing, the raw data must be of reasonable quality to ensure reproducibility and accuracy of the analysis.

3.2 Spectral Imaging Systems for Manuscript Analysis

A typical spectral imaging system consists of three main components: The imaging-unit, the lighting and, if necessary, a movement-unit (portal) that transports either the scanner or the object during data acquisition.

3.2.1 Bandwidth Selection

To select and isolate the wavelengths for each spectral image, different approaches are possible. One is, to filter the light reflected from the object.[11] If the filter is placed in front of the lens-system, the aperture of the filters must be considered. It is therefore more efficient to place a motorized filter wheel behind the lens, that automatically switches the filters. The most important downsides of this configuration are the limited number of spectral bands and the time-consuming data collection process. Tunable filters composed of liquid crystal elements that can be adjusted to filter specific, narrow bands can be used to address these issues.[12] Filter-based MSI systems are usually custom made and designed, including an optimized lighting system and are technically and economically relatively efficient.

By adding a filtering system to the lighting source, the incident light that illuminates the object can be selected. This is one of the earliest approaches to MSI in manuscript analysis.[13] A more recently adapted way of selective lighting has become possible by the advance of LED-lighting arrays with a tunable spectral output.[14] This procedure has several upsides: The selective lighting approach is less stressful for the objects, because only a portion of the EMS reaches its surface. By using cold LEDs, the heating of the object during scanning is very limited. At the same time, modern LED-systems can deliver a stable output at narrow bandwidths. By using pre-defined LED-combinations, an RGB-camera and a standardized calibration system, very cost-effective systems with high spectral and spatial quality are possible.[15] The registration process, on the other hand, becomes more time consuming, the more bands are to be recorded, as the system has to be readjusted and focused for every shot. Such systems are also limited in the number of spectral bands and the spectral bandwidth.

[11] LIANG (2012), pp. 311-312.
[12] HARDEBERG ET AL. (2002).
[13] SAUNDERS/CUPITT (1993).
[14] CHRISTENS-BARRY ET AL. (2009).
[15] SHRESTHA/HARDEBERG (2013).

3.2.2 Hyperspectral Line-Scanning Cameras

A technique of bandwidth selection widely used in remote sensing and machine vision is employing a camera with a two dimensional spectroscopic detector. The diffraction is achieved by a diffractive grating or prism that disperses the light on the scanner, which simultaneously acquires the whole spectral range for each pixel in a line. The scanner, or the object under the scanner is then moved to the next line under the slit, until the whole area of interest is scanned.[16] Most hyperspectral systems are built using this principle. Modern CCD detectors can capture the near UV, VIS, NIR and SWIR (short-wave infrared: Approximately 1,3 to 2,0 µm) regions in a spectral resolution of a few nanometers. A downside is their usually much lower spatial resolution and higher price, compared to photography-based systems.

3.2.3 Lighting

Aged manuscripts are generally highly light-sensitive. It is therefore imperative to select an illumination system that can provide sufficient intensity for high-quality imaging, but also minimizes the lighting dosage and the potential damage to the manuscript. Regarding the dosage it is assumed better to record at high illumination intensity for a short time, than vice-versa, to gain enough signal intensity for the detector.[17]

3.3 Software Packages for Multivariate Image Analysis

There is a variety of open source and commercial software packages available. An overview of some frequently used is given by JENSEN (2016), pp. 125-130. This section presents the software used in this work:

ENVI (Environment for Visualizing Images) is produced by Harris Geospatial Solutions Ltd. It is a widely used software package, originally developed for remote sensing applications. ENVI is based on the programming language IDL, developed in the 1970s by DAVID STERN.[18] It includes a variety of algorithms and workflows that can be exploited for the analysis of multivariate manuscript images and was the main software used in this work.

ImageJ is a Java-based image viewing and processing application. The system is open-source and a variety of plug-ins are available, or could be designed using Java, to enhance its

[16] LIANG (2012), p. 312.
[17] LIANG (2012), p. 310.
[18] http://www.harrisgeospatial.com/Company/AboutHarrisGeospatialSolutions.aspx, last viewed: 21.01.2018.

capabilities.[19] ImageJ was used to create color-composites for FFT-filtering. It was also used to produce composite false-color images of different greyscale images.

Adobe Photoshop CS5 was mainly used for post-processing the images generated in ENVI. This encompasses contrast and color enhancement, blending of different images and generating composite images.

3.4 Multispectral and Hyperspectral Image Analysis

3.4.1 Multivariate Image Analysis

Multivariate image analysis, the processing and analysis of images containing more than one information per pixel, is a wide field that uses many different types of images and has a variety of scientific applications. The vast amount of data collected by modern spectral imaging systems necessitates algebraic, geometric and statistical transformations to extract the information needed. This is achieved by transferring the information into a form, that is better interpretable by a human operator or a machine learning algorithm. Multivariate image analysis roughly comprises three steps: Data pre-processing is a prerequisite of image analysis that increases the image quality and statistical coherence. Image/Information compression is used to lessen the amount of redundant information in the image. In the image analysis step, the data-cube is analyzed according to the analytical goal. This process includes, for example, image classification and segmentation.[20]

3.4.2 Multivariate Image Statistics

Multiband images can be characterized using low-order statistic measures like mean, maximum and minimum, variance and standard deviation of the individual bands. While such statistics are useful to estimate tendencies and dispersion in the band images , they do not well describe interrelation between the bands, for example, whether the bands variation is connected or independent. Important second-order statistical concepts are covariance and correlation.

Covariance describes whether the reflectance value of a pixel in different bands changes jointly. A high positive covariance indicates that if band x has a high variance, a high variance for band y can be expected. If negative, the factors vary inversely. A value close to zero expresses a very low covariance.

[19] SCHNEIDER ET AL. (2012).
[20] PRATS-MONTALBÁN ET AL. (2011), p. 2.

Correlation represents the standardized covariance. This standardization normalizes for a data set with strongly varying values, like, for example, if the input contains data from multiple sensors with differing units or intensity-values. Correlation is a unitless ratio with values between -1 and 1.

One important concept is the **variance-covariance matrix**. This symmetric matrix lists the bands individual variances on the diagonal and the covariances in all possible band combinations off-diagonal (table 1). The variance-covariance matrix (and, analogously the correlation matrix) is utilized by various methods to estimate unknown parameters of a statistical model and thus an important basis for many algorithms. [21]

Table 1: Simple covariance- and correlation-matrices, calculated for the three-banded photograph in figure 1, showing very high positive covariance/correlation and strongly differing variance among the bands.

Covariance	Band 1	Band 2	Band 3
Band 1	144.224	184.424	225.509
Band 2	184.424	256.515	333.970
Band 3	225.509	333.970	458.005

Correlation	Band 1	Band 2	Band 3
Band 1	1	0.958	0.877
Band 2	0.958	1	0.974
Band 3	0.877	0.974	1

3.4.3 Redundancy in Hyperspectral Image-Data

The examination of neighboring spectral bands shows, that many of the band images appear almost identical. Since the intensity of the reflection of most materials in the VIS-NIR-region varies only gradually, most bands share a large amount of information. Therefore, hyperspectral images can usually be expected to be highly correlated and redundant. The strongest correlation appears in blocks of neighboring spectral bands which is also apparent in typical VIS-NIR reflectance spectra of most materials, showing only gradual change over larger ranges and strong changes between these similar areas. While MSI can be explored visually, by examining the bands one after the other, the high number of bands in an HSI make it less readily explorable. On the other hand, the high redundancy enables to design statistical models that can predict new features based on statistical relationships in the large dataset. This can be utilized in automated labeling of unlabeled data (classification).[22]

[21] JENSEN (2016), pp. 138-141.
[22] RICHARDS/JIA 2006, pp. 359-363.

3.4.4 Data Visualization and Information Fusion

Image fusion is a common task in many imaging applications like remote sensing[23] and medical imaging[24]. Image fusion methods aim to combine the relevant information from different sensors or images into a grayscale, or multiband image, which is more suited to answer the analytical task.[25] Depending on the application there are different goals of image fusion: Combining the information about an object or location from different sensors, increasing the spatial or spectral resolution of an image, or to find obscured patterns and structures in the data by statistical analysis.

In the case of spectral imaging experiments on palimpsests, many researchers rely on false-color imaging, where a new color image is created by using different bands as input for the RGB-channels, to form a full color image in combination. By combining the information of selected bands, the contrast between materials can be modulated to enhance readability. If the inks are transparent in different spectral regions, the channels can be chosen accordingly to produce an image showing only selected inks. One example is the so-called pseudocolor-method, developed for the analysis of the Archimedes Palimpsest.[26] To better separate the writings, the green and blue channels are both filled by an UV-blue image. The red channel stays the same. In the case of the Archimedes Palimpsest this led to a grey-colored overtext and a reddish undertext. These approaches are limited by the three channels, perceivable by the human eye, but also by the available dataset. Only if there are bands available that show the desired features already clearly enough, the combination will provide enhanced visibility. Since most imaging experiments use multispectral data with usually less than 20 spectral bands, the band combination process is much more feasible than with hyperspectral data, where the optimal bands are difficult to find in the large data set.

More images can be incorporated by standard mathematical operations (add, subtract, divide, multiply) or more complex blending operations. Adobe Photoshop[27] implements 26 different blending operations that can be combined using the layer structure of the package. Still, the combination of too many layers will reduce contrast, sharpness and clearness of colors and thus hinder an easy interpretation. For this reason, blending and composition techniques are most applicable if only around three images are fused. If used with suitable input, color

[23] GHASSEMIAN (2016).
[24] JAMES/DASARATHY (2014).
[25] GRIFFITHS (2015), pp. 364-365.
[26] EASTON/NOEL (2010), pp. 65-66.
[27] Adobe Photoshop CS5, Adobe Systems Software Ireland Ltd., Dublin, Ireland, 2014.

composite images provide intuitively understandable combinations of the important information of each image.

A variety of algorithms have been developed that can optimize the fusion process. Most techniques are based on a transformation of the data, that extracts and combines the valuable information from each image. Wavelet- and pyramid-based methods are often used means of image fusion. Their application on manuscript image enhancement is discussed by GRIFFITHS (2015), albeit using multispectral data. In practice, the method of information fusion depends on the spectral properties of present materials and the goal of the fusion process. Possible transformation methods to fuse one or multiple hyperspectral image-cube include dimensionality reduction methods, like principal component analysis (PCA), that automatically assemble the most relevant information in fewer bands. The most important methods of this type will be explained in the following chapter of this work.

3.4.5 Transformation

As mentioned above, digital images (including multiband images) are readily describable in mathematical terms. This allows for mathematical operations to be applied for the analysis. Transformations can be applied in order to enhance spectral features of relevance (for example the contrast between text and background), or to reshape the data to become easier to process for analytical algorithms (for example by filtering for classification-relevant features). Transformation processes can be classified into point operations that affect every pixel value independently and local operations that modify pixel values in relation to their surroundings.[28] The data can be transformed according to many different principles with the most important in this context being: Spatial filtering and dimensionality reduction methods.

3.4.5.1 Spatial Filtering

Filtering in the spatial domain applies a moving window or kernel of defined dimensions to modify the pixel values in relation to the local area under the window. Each pixel under the kernel is modified by a predefined value before the kernel is moved by one pixel and the operation repeated. Such local operations enhance or attenuate features of spatial frequency. This is achieved by assigning each element in the kernel a specific value, depending on the application. Spatial frequency describes the rate and magnitude of brightness changes between neighboring pixels. High-frequency indicates a rapid and drastic change in brightness for example in a strongly textured area. Applying a low-frequency or low-pass filter may be used to attenuate high-frequency changes for noise-removal or smoothing operations. Here, the kernel (convolutional mask) is designed to flatten the brightness in the local area. High-

[28] JENSEN (2016), p. 273.

pass filtering may be used to enhance high-frequency features which sharpens the image.[29] ENVI, Image J and Photoshop all implement different convolutional filters and also allow the user to define new filter-kernels.

3.4.5.2 Dimensionality Reduction

By applying a dimensionality reduction transformation, a new set of images is generated that enhances specific features of the data while suppressing redundancy. This can be used for visualization and data-reduction. Two main types are differentiated: Feature extraction and feature selection methods. Feature extraction methods are unsupervised and therefore find relevant features in the unlabeled data automatically. Feature selection requires the user to pre-label the classes.

Since much of the spectral information can be considered redundant, a significant compression of the data can be possible, without losing the relevant information concerning the analytical question.[30] This has benefits to the computational expanse and the performance of subsequent computations. If the information is spread in an unnecessarily high dimensional space, the relevant information can become diluted. This is the so-called “curse of dimensionality” – the exponential increase of space in high dimensional systems.

The problem of dimensionality reduction can generally be defined as follows: For a random n-dimensional image vector $x = (x_1, \dots, x_n)$, find a lower dimensional representation $s = (s_1, \dots, s_k)$ of the vector with $k \leq n$ while conserving the information relevant to the analysis.[31] The components of vector x are called attributes, those of s are called hidden variables.

Linear dimensionality reduction methods assume that the observed vector x is a linear combination of hidden variables s, weighted by the linear transformation weight matrix W:

$$X = Ws$$

The projection-criteria are estimated from the second or higher order statistics of the observation matrix X.[32] In other words, dimensionality reduction methods search to determine underlying hidden variables in the data, by analyzing the statistics of the observed matrix. Then, a linear transformation can be found, that reprojects the data onto fewer axes (dimensions) to make the hidden features more accessible and reduce redundancy. Which feature-extraction parameter is chosen defines the dimensionality reduction technique.

[29] JENSEN (2016), pp. 293-302.
[30] RICHARDS/JIA (2006), pp. 136-137.
[31] FODOR (2002), p.1.
[32] NUZZILARD/LAZAR (2010), pp. 242-244.

Often applied linear dimensionality reduction methods include principal component analysis (PCA), minimum noise fraction transformation (MNF) and independent component analysis (ICA) among many others.

3.4.5.2.1 Principal Component Analysis (PCA)

PCA is one of the most applied linear transformation methods. PCA projects the data onto new sets of axes by translation and/or rotation of the original axes, to run along the vectors of highest covariance in the data. This transformation maximizes variance and eliminates correlation between the transformed images (or principal components - PCs).

First the covariance matrix of the image matrix is computed. Then, the data is projected along new axes formed by the eigenvector matrix of the covariance matrix. An eigenvector of a matrix is a vector that, if multiplied by the matrix, does not change its direction but only its length. The value of scaling is defined as eigenvalue. The higher the eigenvalue, the higher the covariance along the vector. By using the eigenvectors as new (orthogonal) axes, the principal components (*S*) of the observed matrix (*X*) and the eigenvector matrix (*B*) are formed: [33]

$$S = BX$$

The transformation coefficients and thus, the transformation result, are derived from the statistics of the original data. The number of PCs found equals the number of variables of the input data. The algorithm sorts the PCs by decreasing eigenvalue. Since the PC-axes follow the directions of highest covariance, the first PCs also contain most of the variance in the image and are therefore most likely to contain the most relevant information of the image-cube.

Since the transformation is linear, a reverse-transformation is possible. By leaving out the less-contributing components the redundancy can be reduced. These components have only very limited influence on the parameters of the reverse-transformed data and the resulting pixel values and therefore, on the amount of information. The PC-transformation and reverse-transformation also enables a variety of methods to pre-process and improve the image-cube for the subsequent analysis, for example noise reduction, image fusion and spectral sharpening. Some of these methods are also useful for the readability enhancement application and will be explained in later sections of this work.

PCA can thus be used for different benefits:

- Fusion by substitution of components and inverse-transformation
- Selection of an optimized band-set

[33] NUZZILARD/LAZAR (2010), p. 244.

- Image enhancement by selective removal of noisy bands
- Feature extraction

In the case at hand, PCA is mainly used to concentrate the relevant information into fewer dimensions to improve the effectiveness of subsequent classification. The PCA images can be used to visually identify important clusters in the image and to find suitable training points for machine learning algorithms. Since the PCs will often concur with different types of materials, the PC-images can enhance the contrast between materials and therefore display an enhanced readability of faded or erased scriptures. PCA was used successfully in numerous readability enhancement experiments, for example, on the Archimedes Palimpsest.[34]

3.4.5.2.2 Minimum Noise Fraction (MNF)

MNF is a linear transformation designed to separate noise and information in an image. While PCA maximizes variance, MNF is designed to enhance the signal-to-noise ratio, and therefore the image quality, especially in HSI.[35] Since most of the noise present in the image stems from the scanner or the scanning process, it is assumed that the image noise is normally distributed and not correlated to the signal (the information of interest). The intensity value Z at each point x is composed of the signal S and the added noise N:

$$Z(x) = S(x) + N(x)$$

Under the assumption of uncorrelated signal and noise components, the images covariance matrix can be expressed as the sum of the covariance matrices of signal $\sum_S$ and noise $\sum_N$:

$$cov\,\{Z(x)\} = \sum = \sum_S + \sum_N$$

MNF uses the covariance matrix of the noise components to find linear transformations that maximize the noise variance in each band. By this, the noise gets decorrelated and normalized over all dimensions. This step is called whitening of the noise and can be described as a standardized PCA of $\sum_N$. Since the noise value is usually unknown it has to be estimated in the process using the eigenvectors of the noise covariance.[36] Then, the noise-whitened image is transformed using PCA. This results in a PCA-like transformed image, only that the MNF will selectively separate the (de-correlated) noise from the signal-containing bands. The output bands are sorted by decreasing image quality with the first components having the best signal-to-noise ratio. The image can then be reverse-transformed after excluding or filtering out noisy bands, resulting in considerably reduced image noise. This is especially effective if strong

[34] EASTON/NOEL (2010), pp. 71-74.
[35] CANTY (2014), pp. 111-112.
[36] GREEN (1988), pp. 65-68.

systematic noise from the scanning process is present, but also white noise is filtered effectively.

3.4.5.2.3 Independent Component Analysis (ICA)

As well as PCA, ICA was used successfully in readability enhancement on the Archimedes Palimpsest.[37] ICA is considered a powerful method to solve the blind source separation problem (BSS). This problem describes the unmixing of simultaneously recorded signals from different sources. A popular example is the so called “cocktail party problem”: Different people speaking at a party are recorded by two microphones at the same time. Both microphones register a linear mixture of the different voices, background sounds and music, weighted only by their distance from the respective sources. The BSS tries to recover the original signals from the linear combinations recorded. A tutorial to ICA is provided by SHLENS (2014). While the key assumption behind PCA is, that the recorded data is a linear combination of uncorrelated components, ICA assumes statistical independence between the original sources, that linearly contribute to the observed signal. Statistical dependence is, like covariance, a measure of joint variation, but from a standpoint of probability theory. Two variables a and b are statistically independent, if the occurrence of one does not influence the probability of the other. In this case, the joint probability $P\ (a, b)$ is equal to the product of the probabilities of each variable occurring:

$$P(a, b) = P(a)P(b)$$

In the BSS scenario, the joint signal probability $P(S)$ is equal to the product of probabilities of any possible combination of signal probabilities $P(s_i)$:

$$P(S) = \prod_i P(s_i)$$

The main problem of ICA can be formulated as

$$X = WS$$

with X being the observation, S the independent sources and W an unknown mixing factor. Independece is a much stronger condition than uncorrelatedness. Thus, higher-order statistics than PCA (which only uses the covariance-matrix) are needed, to find a transformation that ensures statistically independent components. The linear projections are, in contrast to PCA, not necessarily orthogonal (figure 4).[38] This allows ICA to find and isolate features, that PCA is unable to detect. ICA is a computationally intense method. It is therefore practical to reduce

[37] SALERNO ET AL. (2006).
[38] NUZZILARD/LAZAR (2010), p. 244.

the dimensionality by PCA or MNF and apply ICA on the most relevant bands. This can also prevent from results impaired by image noise.[39]

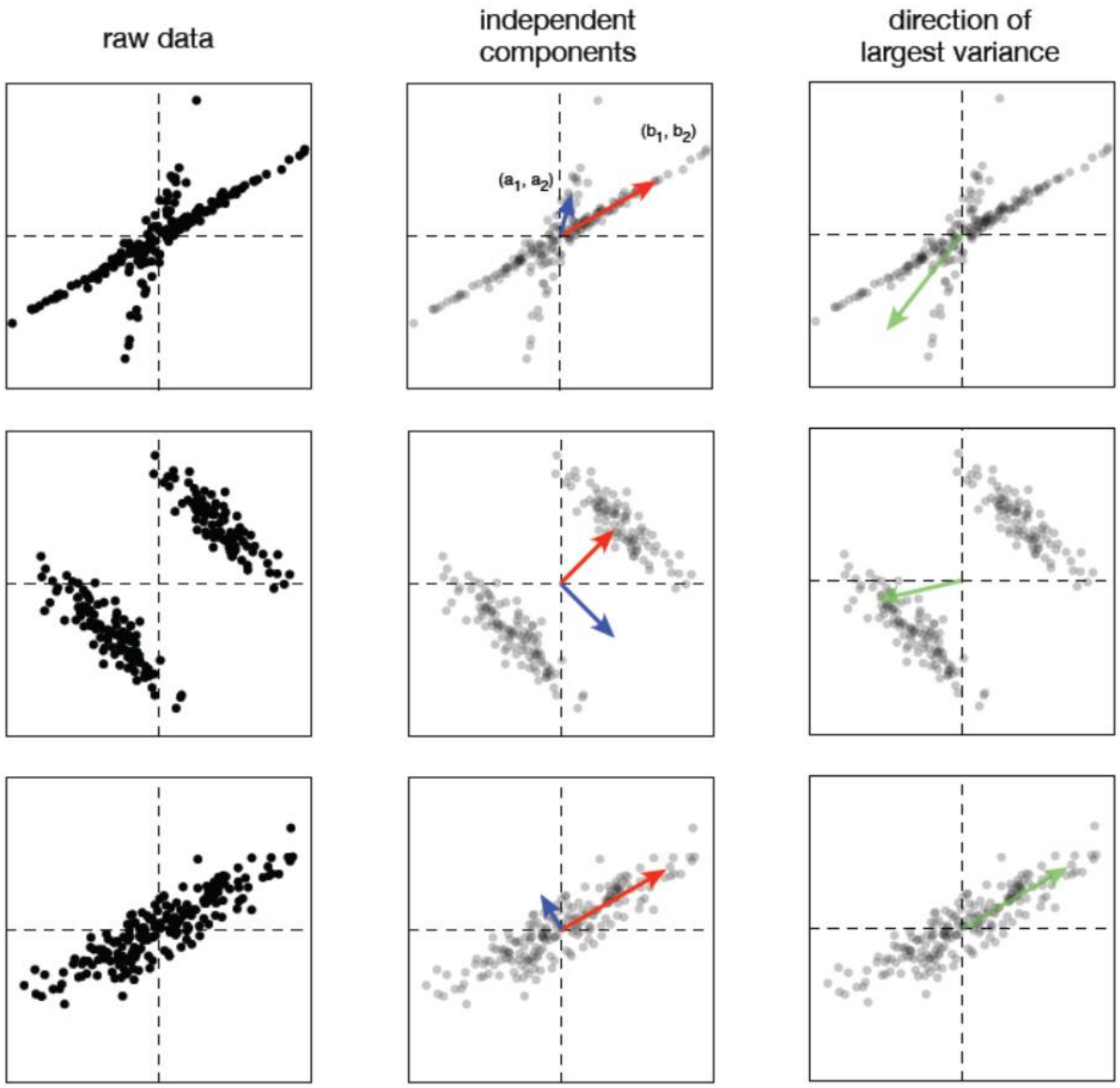

Figure 4: Two-dimensional, linearly mixed datasets (left), the directions of the independent components (middle), the direction of largest variance (right). The independent components are not necessarily orthogonal. Image reproduced from SHLENS (2014), p. 3

3.4.6 Spectral Classification

Classification is the process of sorting unlabeled data into a number of predefined or previously unknown classes, carried out by a classification algorithm. Supervised classification uses class labels, or training data, set by the user. Unsupervised methods try to find class labels without

[39] TONAZZINI ET AL. (2004), p. 20.

any preceding knowledge and classify every pixel into one (or more) of the established classes. This work will focus on supervised classification methods, since classification is considered to deliver better results, if class-knowledge is available.

3.4.6.1 Supervised Classification

There are many algorithms available to solve different forms of classification problems. Among others, ENVI implements the following, well documented classifiers: Minimum distance classification (MinDC), maximum likelihood classification (MLC) and mahalanobis distance classification (MaDC). The following basic steps of classification in our context apply to all these methods:[40]

1. Definition of the classes in which the image should be segmented (for example: background, undertext, overtext, stained areas, bled-through ink, etc.)
2. Selection of pixels to be used as training data. Estimation of the statistical parameters from the training data to train the classifier to execute the classification.
3. Execution of the classification. The classifier labels all pixels in the chosen subset based on the decision rules learned from the training data.
4. Creation of a thematic class mapping that visualizes the classification results.
5. Examination of the result based on regions with sufficient visibility for manual labeling.

Classifiers can be grouped by different criteria. One factor is the learning process that defines how the classification rules are established. MLC and MaDC classifiers use the covariance-matrix of the training data to estimate a function of probability, whether to expect a pixel x to be a member of a predefined class M, assuming the probability to be normally distributed. The pixels are labeled to the class with the highest probability. The MinDC is a mean-centered classifier that calculates the mean-vector of the training data in each band and then clusters the image pixels by measuring the distance of the pixel vector to the different class-means. The algorithm then labels the pixel to the class with the shortest mean-distance.[41]

3.4.6.2 Training Samples and Classification of Hyperspectral Data

The selection of samples used to train the classifier is of high importance for the classification result and also depends on the chosen classifier. While MinDC only requires a small number of training points to estimate the mean vectors of the classes, MaDC and MLC require much more training data to estimate the covariance matrix of M correctly. As a rule of thumb, a

[40] RICHARDS/JIA (2006), pp. 193-194.
[41] JENSEN (2016), pp. 395-402.

number between $10N$ and $100N$, with N being the number of spectral bands is advisable.[42] Besides the classifier-specific requirements, a larger training data set generally leads to more reliable classification. Since the separation rule is computed based on the training data, a more accurate separation is possible if more points are given, as shown in figure 5.

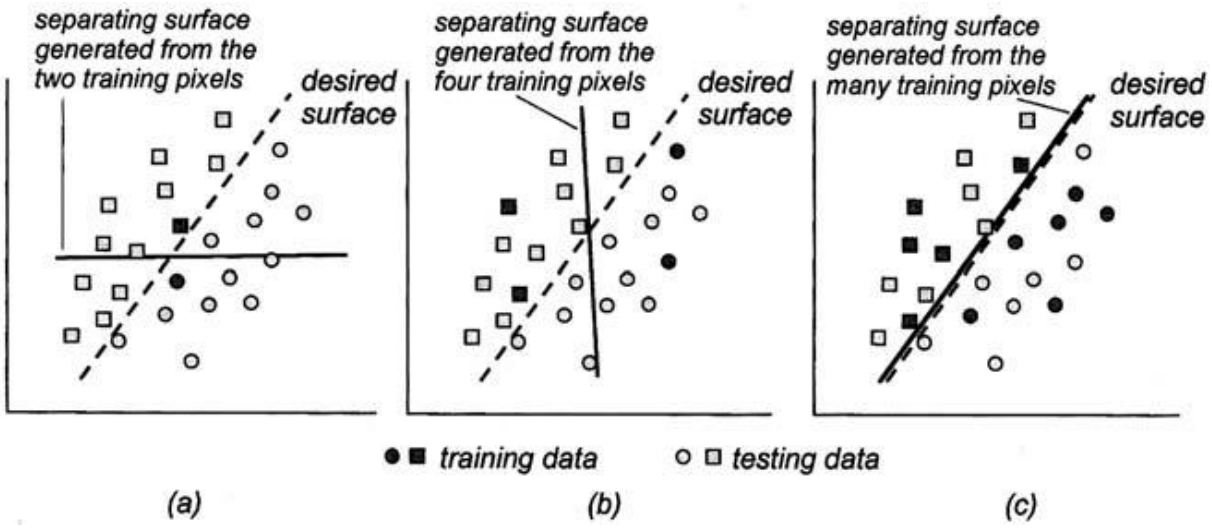

Figure 5: The significance of training point number on class-separation. Image reproduced from RICHARDS/JIU (2006), p. 365

A hyperspectral data set with more than 100 bands would need between 1000 and 10000 points, according to this rule. Such a high number of reliable points may be hard to find for sparser classes.[43] This indicates, that hyperspectral data sets can necessitate a different approach to classification. One apparent method is dimensionality reduction. If the unreduced dimensionality is to be used, a frequently applied method is the spectral angle mapper classifier (SAM). This method does not use class-statistics, but performs labeling based on the pixel vectors direction in n-dimensional space. Each image vector forms an angle with the reference-vectors and can be classified to the class with which it forms the smallest spectral angle. This makes SAM more prone to the problem of insufficient training data. The disregard of class-covariance, on the other hand, makes it less capable of classifying points in a strongly varying dataset. For each given reference spectrum, the algorithm creates a new image showing the difference in the spectral angle between the pixels and the reference as grey-values. Thus, a new stack of SAM-images is created, that can be thresholded to produce a classification map.[44] [45]

[42] RICHARDS/JIA (2006), p. 199.
[43] RICHARDS/JIA (2006), p. 364.
[44] JENSEN (2016), pp. 479-480.
[45] RICHARDS/JIA (2006), pp. 368-369.

3.4.6.3 Matched Filtering and Target Detection

Another important group of methods that has been proven useful for manuscript improvement is matched filtering. A matched filter (MF) searches the image-cube for a user-defined target in an unknown spectral background (target detection). This target is defined by its spectral characteristics and, if available, the class statistics of the training data. Seeing each pixel as a weighted combination of different signals, MF seeks to find and maximize the targets contribution to each pixel. The output can be in form of an abundance map with the pixel brightness corresponding to the relative abundance of the target in the pixel. This mapping can then be thresholded to produce a classification image. As opposed to the supervised classification algorithms presented above, a target detection method assumes a relatively low abundance of the target in the scene, with a much higher contribution by an unknown background. This parallels the problem of faded or erased inks on parchment or paper.

A target detection workflow proposed by JIN ET AL. (2009) is implemented in ENVI and supports eight target detection methods. Among these, adaptive coherence estimator (ACE), spectral angle mapping (SAM) and constrained energy minimization (CEM) have already been successfully applied for processing spectral images of faded manuscripts.[46] SAM was already discussed above in its function as classifier. SAM is assumed to be a robust multi-purpose method, that, since it does not depend on large training sets, is also applicable as a target detection method where it has the same advantages and limitations as explained above. ACE and CEM are related methods that try to maximize the target-response while minimizing the background. Both use the covariance/correlation matrix of the training data to estimate the probability of target detection in each pixel. ACE is invariant to scaling of the training data and has a constant false alarm rate, which makes it more prone to false-detection. [47] Another possible advantage of ACE is, that it finds a non-linear transformation of the image, which can result in better results, if the classes are non-linearly related. This could aid in the separation of very similar inks.[48] An unsupervised form of target detection is anomaly detection. Anomaly detection has no a priori information about the scene and tries to find possible anomalies by comparing them with their surrounding pixels, or the entire dataset. The most important anomaly-detection algorithm is the rx-algorithm.[49]

[46] GRIFFITHS (2011), HEDJAM ET AL. (2014), HOLLAUS ET AL. (2015/2).
[47] JIN ET AL. (2009).
[48] HOLLAUS ET AL. (2015/2), p. 112.
[49] REED/YU (1990).

4 Applied Hyperspectral Imaging and Multivariate Image Processing

In the following, multispectral and hyperspectral imaging techniques were applied on different historic manuscripts to enhance the legibility of faded or deliberately removed writings. After an introduction into the hyperspectral imaging system used, and the pre-processing steps that were applied, three examples are presented that show the applicability of spectral image processing to different, often encountered issues concerning historic manuscript readability.

4.1 Data acquisition and Pre-Processing

4.1.1 The Imaging System

Figure 6: The hyperspectral imaging system of the BSB

The hyperspectral imaging system of the BSB that was used in this work consists of the following main components: The imaging-spectrometer, the illumination-unit and the portal-unit. The imaging-spectrometer unit consists of the hyperspectral camera the spectrometer and optical lenses. Two imaging-spectrometer systems, covering the combined spectral range of around 400 to 1700 nm are employed. The VNIR scanner utilizes an Adimec A-1000 VNIR

camera [50], a Hyperspec VNIR hyperspectral spectrometer [51] and a VNIR-corrected lens [52]. The system captures the spectral range of 328 nm to 1055 nm in 250 spectral images with an approximate bandwidth of 3 nm and 1004 horizontal pixels per scanned line. The NIR scanners components are: A Raptor Owl 320 HS NIR-camera [53], a Hyperspec NIR hyperspectral spectrometer [54] and a NIR-transmissive lens[55]. The scanner has 320 active pixels per line. It covers the NIR between 918 and 1775 nm in 182 bands with an approximate spectral bandwidth of 5 nm. The illumination is provided by 6 halogen spots that are positioned in an ulbricht-tube diffusor. The portal-unit moves the imaging-spectrometer into scanning position and during the scanning process with a maximum precision of 0.1 mm. The system was custom-designed by Fraunhofer IWS (Dresden, Germany). For documentation, reference, and the spectral sharpening process that will be described in the next chapter, a digital SLR-camera (Nikon D300 S, 12.3 Megapixel) was used.

4.1.2 Pre-processing

4.1.2.1 Image registration

If a combination of multiple images is to be used, the images must be aligned precisely. Since ENVI is designed primarily for the analysis of aerial or space-borne images, it relies on geospatial information to register the images to a geographic coordinate system. Satellite-images are usually delivered in combination with accurate coordinates to find the specific location and register the images to a standard raster (geo-referencing). This system can be used for the registration of the manuscript by assigning pseudo-coordinates (x=1, y=1). Every point in the image stack can then be precisely defined by its X and Y coordinates. The different resolutions are reflected by the raster-size of each image, given by the pixel sizes.

After setting up the reference coordinate system, the images can be registered using the image-to-image registration workflow embedded in ENVI. The workflow uses several user-defined tie-points to define a warping function. Based on the point-to-point deviance, the system automatically finds additional tie-points in both images up to a pre-defined number. The NIR and RGB images were warped to match the VNIR image. Because parchment reacts to the temperature increase during the scanning process, the different scans needed to be warped multiple times to achieve satisfying results. The RGB-photograph was additionally pre-

[50] Manufactured by Adimec, Eindhoven, The Netherlands.
[51] Manufactured by Headwall Photonics, Bolton MA, USA.
[52] Manufactured by Schneider-Kreuznach, Bad Kreuznach, Germany.
[53] Manufactured by Raptor Photonics Ltd., Larne, Northern Ireland.
[54] Manufactured by Headwall Photonics, Bolton MA, USA.
[55] Manufactured by Edmund Optics, Barrington NJ, USA.

warped using the Adobe Photoshop CS6 software to correct for the different sensor positions and perspective and optical aberrations. To form a single data-cube the VNIR and NIR-scans were stacked, after spectral ranges with insufficient quality were excluded. This combined image-stack holds all the acquired spectral information from both scanners: 338 spectral bands ranging from 400 to 1650 nm with a spectral resolution of 3 nm in the VIS-range and 5 nm in the NIR-range (table 2).

Table 2: Summary of the acquired image cube

image cube	bands	spectral range	spectral resolution
VNIR	189	400.80 … 949.90 nm	2.9 nm/band
NIR	148	951.20 … 1652.30 nm	4.7 nm/band
RGB-camera	3	~ 400 … 700 nm	~ 100 nm/band

4.1.2.2 Noise Reduction

To improve the SNR, MNF can be applied as a noise reduction method. Especially the NIR-cube exhibits random and systematic noise that impairs the analysis. If used in the following examples, the MNF was applied as implemented in ENVI. After examining the eigenvalues of the transformation, around 30 MNF-bands were used in the inverse transformation, thus preserving more than 90% of the images variance. The noise removal effectively increased the SNR which is obvious in the comparison of spectral profiles before and after the step. The pre-processed spectra are smoother and spectral characteristics are more apparent. This also has positive influence on the visual appearance of the band images. Without random noise the spatial features become sharper and richer in contrast.

4.1.2.3 Spectral Sharpening

Although the de-noising provided a much clearer image, the spatial resolution is still deemed insufficient for the analysis of the finer details of the different scriptures. Therefore, a spectral sharpening step was introduced in the imaging process to enhance the spatial resolution. Spectral sharpening is a sub-category of image fusion. These techniques were developed to improve the spatial resolution of multispectral satellite images by fusing them with a high-resolution panchromatic image[56] (which led to the frequently used term pansharpening). In the process, the high spatial resolution of a Pan-image is injected into a high-spectral-resolution image to generate a MS image with high spatial resolution. Because imaging spectrometers with high spatial resolution are much more expensive, modern satellites often acquire Pan and MS/HS images simultaneously, to allow for a pansharpening step in the pre-processing. Since

[56] Panchromatic image: grey-scale image with constant sensitivity in the VIS-spectrum.

most of the published spectral imaging experiments on palimpsests employ multispectral imaging based on high-spatial-resolution photography systems, spectral sharpening is not an actively discussed topic in this specific field. DURADO-MUNOZ ET AL. (2017) applied the NNDiffuse algorithm to sharpen hyperspectral images of the historic Gough Map of Great Britain.[57] Through spectral sharpening, HS images with lower spatial resolution can potentially achieve almost the same quality while maintaining the higher speed and spectral resolution, which can turn them into viable tools for the analysis of unreadable manuscript texts. The spectral sharpening process will be detailed in the following. It can be mathematically defined as follows:

$$\widehat{M} = \widetilde{M} + \alpha \ddot{P}$$

with $\widehat{M}$ being the result of the sharpening process, $\widetilde{M}$ representing the upscaled MS/HS image and $\ddot{P}$ the details extracted from the panchromatic image. α Controls the fraction of features to be injected. This last factor is necessary to correct differences in spectral sensitivity of the different sensors.[58] KHAN/CHANOUSSOT (2010) name three categories of pansharpening techniques:

Component substitution (CS) based methods, multiresolution analysis (MR) based methods and hybrid methods. The main difference between CS and MR lies in the method of extraction of the high-resolution features from the Pan image and their injection into the MS/HS image. While MR methods make use wavelet decompositions or Laplacian pyramids to extract and reinsert the information, the CS methods use various image transformations to combine the Pan image with the transformed MS/HS image and fuse their spatial and spectral information by reverse transformation. The selection of a spectral sharpening algorithm depends on the image characteristics, the analytical objective and other factors like computational expense and the amount of necessary pre-processing. ENVI implements different well-established algorithms like principal component pansharpening or Gram-Schmidt pansharpening among others, and the more recently developed Nearest-neighbor diffusion pansharpening (NNDiffuse).[59]

One important weakness of most of these algorithms for the here discussed application is, that the methods are all originally designed to sharpen multispectral data with approximately the same spectral range as the pan image. There have been various proposals for spectral sharpening algorithms designed for the fusion of hyperspectral data that exceeds the range of

[57] DORADO-MUNOZ ET AL. (2017).
[58] KHAN/CHANOUSSOT (2010), p. 58.
[59] SUN ET AL. (2014).

the pan image.[60] These methods rely on different transformation and interpolation techniques to transfer the established practice of pansharpening to hyperspectral data but are not yet available in the ENVI package. While all methods experience shortcomings and advantages, CS-methods are generally less complex and computationally intense and more prone to slight misalignments between the input images. The last being especially important since the pan and HS-image were not taken from the exact same position. Also, due to the slight movement the parchment exhibits during the imaging process, the images are not assumed to be perfectly aligned. Since the NNDiffuse sharpening algorithm used by DORADO-MUNOZ ET AL. (2017) requires especially well aligned images, and due to its inferior performance in preliminary tests, a different algorithm was searched for.

PC-sharpening is a relatively straightforward sharpening method which is based on PCA. PCA is not limited to multispectral data. Also, the possible slight misalignments did not significantly constrain image quality. Thus, PC-sharpening was used to enhance the spatial resolution of the HS image. The process can be outlined as follows: First the HS image is upscaled to the panchromatic image so that both pixel raster are identical. Then PCA is performed on the HS image. The first component (PC-1) usually contains most of the spatial information. PC-1 and the pan image are histogram-matched to equalize differences in the spectral fidelity. Then the PC-1 of the HS image is replaced with the adjusted Pan image and a reverse PCA transformation is applied, to fuse the spatial and spectral information.

PC-sharpening tends to introduce spectral distortions to the MS/HS image which in the RGB-composite appear as shifted colors. This is due to the use of a pan image as substitution. The 1st PC contains mostly high-frequency information, while the Pan image also carries low-frequency information that is responsible for the distortion.[61] To address this issue, the high resolution photograph was PCA transformed and the first PCA-band used as high resolution input, instead of a pan image (figure 7). The VNIR-cube and the photograph share largely the same spectral range and except for the different spatial resolution, the first PCA-bands of both images are identical. The images sharpened in this way showed no distortion and appeared qualitatively superior and less computationally intense, compared to the other sharpening techniques implemented in ENVI. The processed images showed only insignificant spectral differences from the non-sharpened images: The more saturated colors are amplified and the parchments color has become more bluish. Several spectral profiles of important regions were

[60] LONCAN ET AL. (2015).
[61] KHAN/CHANOUSSOT (2010), pp. 61-63.

compared before and after sharpening. The spectra seem to differ only in their overall intensities while the characteristic shape was retained.

The NIR-cube falls outside the range of the RGB-image and was therefore not included in the spectral sharpening process. To match the different resolutions, the cube can be upsampled in the image registration process to have the same pixel size as the sharpened VNIR cube. The smaller pixel raster can be interpolated from the original using cubic convolution. Cubic convolution uses 16 neighboring pixels to predict the new pixel values. This method does not make use of a high spatial resolution reference but smoothens the sub-pixels through interpolation. Both cubes are stacked to form a single, VIS-NIR-HSI cube.

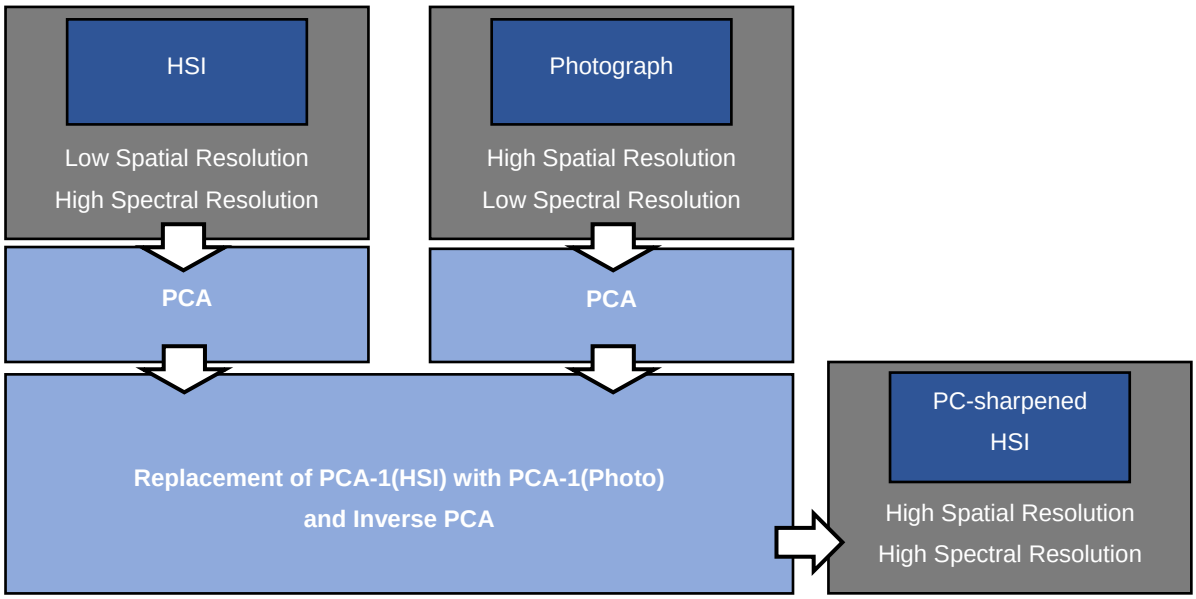

Figure 7: Diagram of the proposed PC-Sharpening workflow

Figure 8: Result of the PC-sharpening of Clm 29416 1-verso, VNIR-cube. RGB-composite image (Red: 640.3 nm, green: 549.8 nm, blue: 470.9 nm) Left: before sharpening, right: After applying the described PC-sharpening method

4.2 Exemplary Applications

4.2.1 Reduction of Recto-Verso Artifacts Using ICA

In some cases, the information of interest is not obscured by overlying, but rather by underlying elements. An often-occurring problem in the analysis of aged manuscripts is ink bleed-through or see-through. Due to aging or insufficient preparation of the paper or parchment, the ink from one side of the manuscript is transported through the paper and appears on the other side. See-through describes a similar effect: If the paper is not completely opaque (or becomes more transparent due to aging) the information of the opposite side will also be visible. While the human eye can often discriminate between the writings, the effect can be fatal for algorithms designed to process the manuscripts automatically, for example optical character recognition (OCR). This makes the topic especially relevant for libraries and archives trying to digitize their collections.

Figure 9: Msc.patr. 5, fol. 1. Co-registered recto- and (mirrored-) verso-side

The codex Msc.patr. 5, preserved in the DNB, contains a famous illumination, showing different steps of manuscript production in a medieval monastery on the verso of folio 1 (figure 9). The recto side however, exhibits deliberately erased text, that is hoped to provide additional information on the genesis and history of the illumination. The text is only barely visible with the naked eye, as brownish shades across most of the recto. High-resolution RGB-photographs of both sides were kindly provided by the DNB and form the dataset for this analysis. The acquisition of a hyperspectral image cube was not possible in this case, but since

most of the methods of transformation, that can be applied to reduce the bleed-through are applicable to both kinds of data, this experiment is also included in this work.

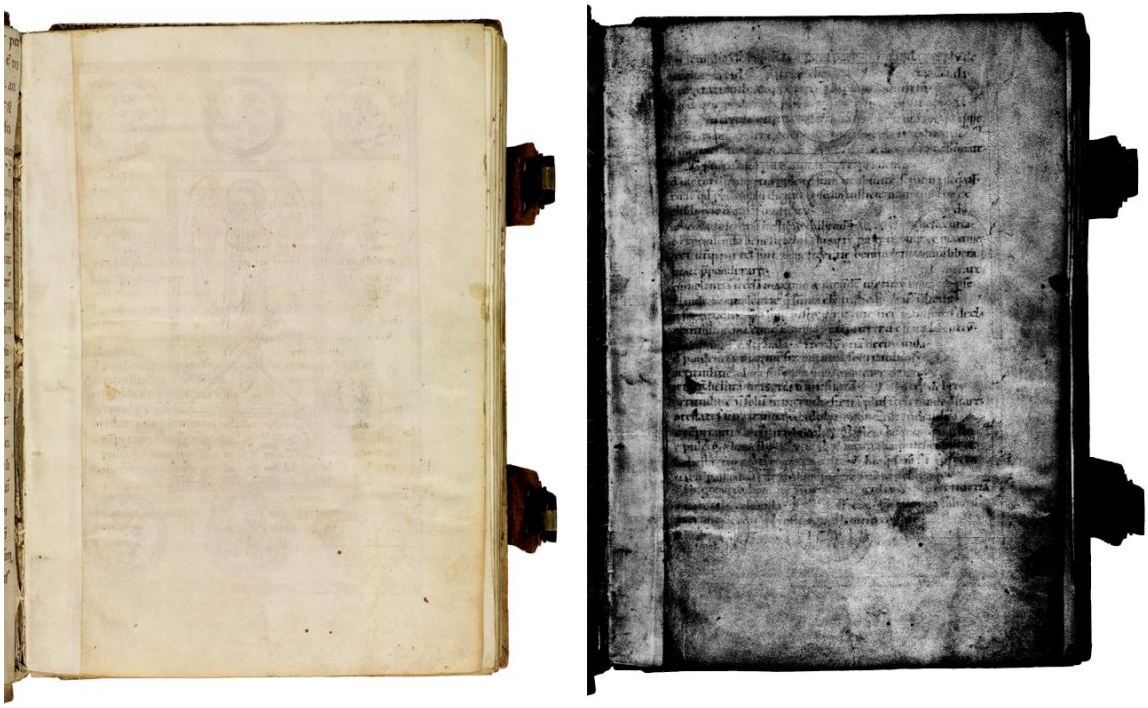

Figure 10: Msc.patr. 5, fol. 1-recto. Left: VIS, right, contrast-enhanced greyscale image of the blue channel. Stains and verso-information are contrast-enhanced as well

One way to enhance features of a photograph is to adjust the images contrast using, for example, the gradiation-curves functions of Photoshop. While the writing becomes more visible by enhancing the contrast, it is difficult to exclusively enhance features of interest. In this case, the visible painting from the verso side is enhanced alongside the text and hinders a clear text visibility in most areas. Thus, the image processing in this experiment is aimed at enhancing the contrast of the faded text while suppressing the misplaced information from the verso-side.

An approach to bleed-through removal as proposed by TONAZZINI ET AL. (2004) was tested in this experiment.

4.2.1.1 Bleed-through Removal by ICA

TONAZZINI ET AL. (2004) formulated the problem of bleed-through removal as a case of blind source separation. In a three band photograph, there are three different observations for each pixel, that can be used, to find the original signals of the classes, that are mixed by an unknown mixture matrix. The bleed through problem is basically a reversal of the palimpsest problem: Instead of trying to enhance hidden features, a way to suppress visible features is sought.

Simplified, both tasks work with the same parameters being “background”, “overwriting” and “underwriting” (or in this case: the drawing from the verso-side), that together constitute the image. By abstracting the problem to three different classes, hidden in three observations (the trivariate image), it fits the basic formulation of the blind source separation problem. [62]

ICA was used without preprocessing on the photograph of the recto, transforming the three channels of the photograph into three independent component images. The three ICs are shown in figure 11. Text and bleed-through are not completely separated into different IC-bands. Most of the text is concentrated in IC-1, except for some letters being visible in the lower left medallion. The bled-through information is spread across all three bands and seems to be composed of two main clusters: One contains mostly sharp lines, that are caused by bleed-through of the red-colored lines from verso, the second relates to the black lines, respectively. ICA separated the classes well, but did not completely remove verso-information from IC-1. Therefor another step is necessary. The brightness-distribution of the verso features in IC-1 is the same as in IC-2, with the red bleed-through in high intensities and the black in low intensities. This enables to erase the remaining verso features by a weighted pixel-by-pixel subtraction of IC-2 from IC-1. Alternatively, this subtraction can be performed in Photoshop, where it is easy to weight the subtraction by changing the transparency of the subtracted image.

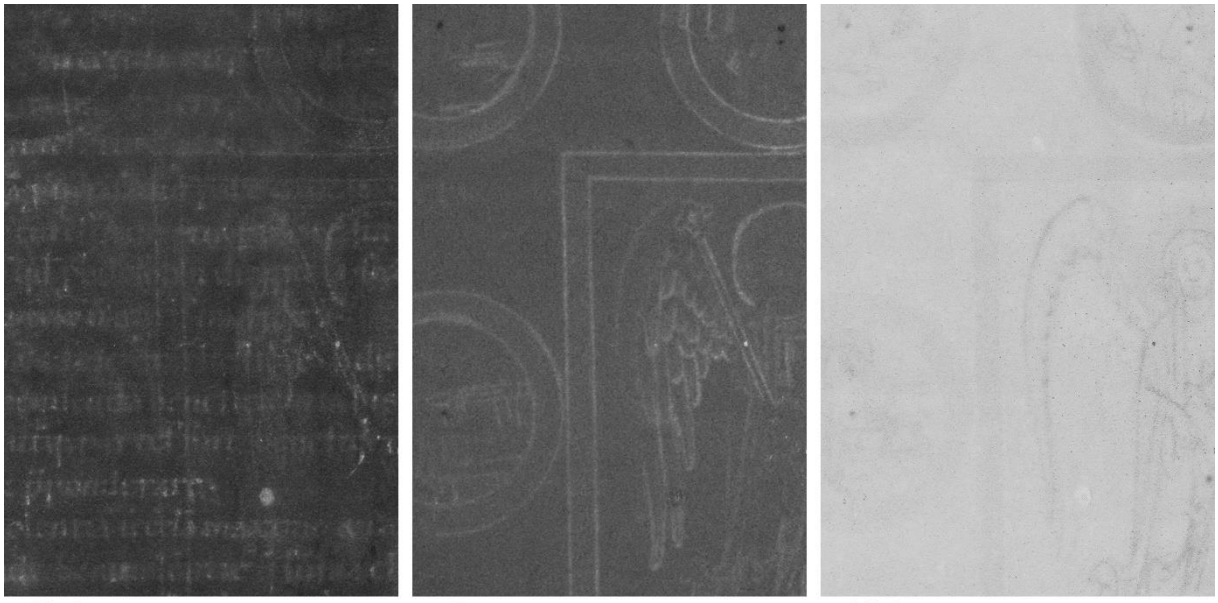

Figure 11: Independent Components of Msc.patr 5, fol. 1, recto

[62] TONAZZINI ET AL. (2004), p. 19.

The subtraction results in an almost complete removal of the bled-through ink. Only in some outlines, for example of the angel's sword, the displaced ink remains visible, but to a much less distracting degree. By adjusting the images' contrast, a much improved readability of the erased text was achieved.

4.2.1.2 Results

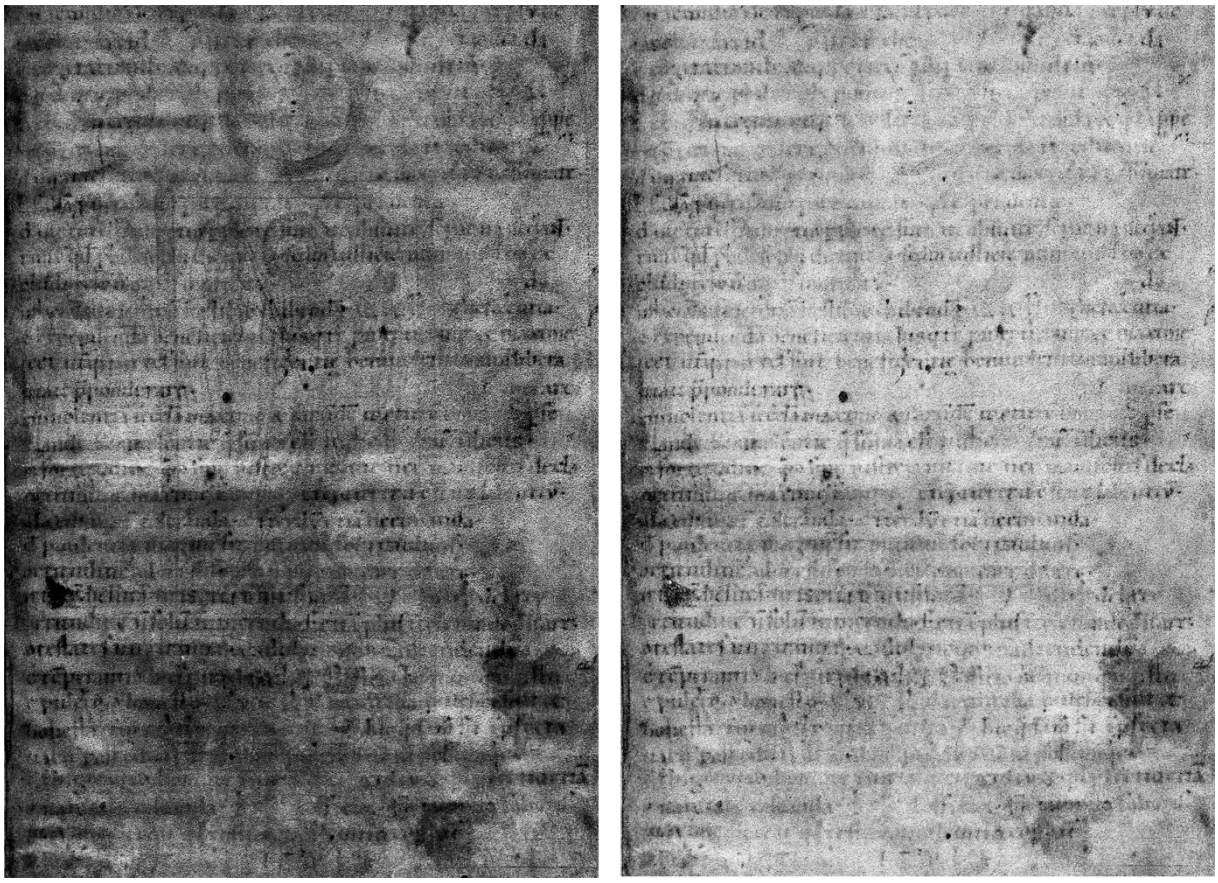

Figure 12: Comparison of the blue channel image of the photograph (left) and the processed image (right)

By combining the ICA bands in Photoshop, a greyscale image almost free of verso-information was produced (figure 12). ICA is able to separate the different classes blindly (without the additional information from the verso), confirming its capabilities as a BSS-technique. An additional possible method would be, to co-register the pages and combine them into a single cube for the separation, but the good results of the ICA-method made this undertaking unnecessary. The provided enhanced image should allow to decipher most parts of the erased text. Additional enhancement would be possible by convolutional filtering to suppress the high-frequency information of the paper-background. Spectral imaging in the VIS-NIR could also improve the visibility further, for example, by enabling to exclude stains and paper texture. A UV-fluorescence photograph may also provide better contrast between paper and ink residues.

4.2.2 Imaging of Covered Writings using NIR-HSI

One well-established application of NIR imaging in is, to make use of the lower absorptivity of paper in the NIR-region to image text, that has been pasted over. Since inks and paints usually exhibit a much higher NIR-absorptivity than paper, it is often possible to image inks through sheets of paper.

This process will be applied to a manuscript of the BSB (shelfmark St.th. 957-2. Figure 13) in this chapter. The manuscript contains historical notes (kettledrum) of the opera "*Götterdämmerung*" by Richard Wagner. One half of page 27 has been pasted over with a sheet showing newer notes. Upon the younger notes some words, notes and lines were written and drawn with a pencil. To make the covered original notes visible again, a hyperspectral NIR-cube of the page was acquired.

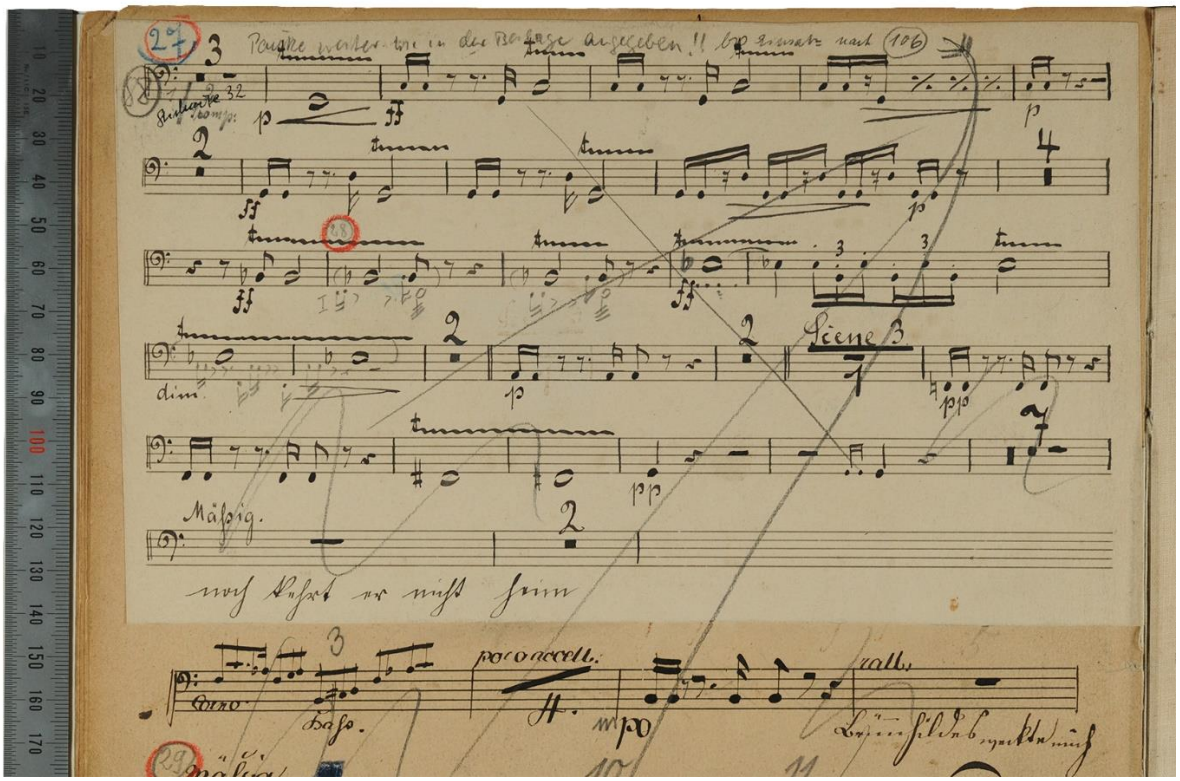

Figure 13: St.th. 957-2: Photograph of the overpasted area

4.2.2.1 Analysis of the Data-Set

The 156 bands containing NIR-cube, spans the spectral range of approximately 950 to 1650 nm. To visualize the different depth of measurement, the image bands can be animated into a video. Starting at 950 nm, the covered notes, lines and different annotations become visible. The best visibility lies in an area between 1050 and 1150 nm. Thereafter the writing becomes more transparent (figure 14). The newer and older notes fade at around 1300 nm

while some annotations remain visible until 1400 nm. Beyond 1400 nm only the highly IR-absorbing carbon of the pencil lines, drawn on the newer paper, remain visible.

4.2.2.1.1 Analytical Goal

As apparent in figure 14, the NIR-images vary strongly with the wavelength. Several writings are visible in different spectral regions, except for the ubiquitous pencil-lines. Since these lines are highly absorbing, they are the most prominent element in all NIR-bands and distract from a clear view of the underlying notes. While the original notes are the information of main interest, the direct comparison of older and newer notes can provide insight into how much was changed and how strongly this affects the music. It was thus deemed of interest to provide an image that contains both, the older and newer notes, as well as all present annotations in sufficient detail and distinctness. The analytical task can therefore be divided into two problems: 1. Fusion of the information into three bands, to visualize all phases of writing in a single RGB-composite image and 2. Reduction of the distracting pencil lines.

4.2.2.1.2 Information Fusion

As the NIR-scan contains high levels of systematic noise (vertical and horizontal stripes), MNF was deemed the appropriate means to reduce the dimensionality and fuse the information into fewer bands. MNF was proven to be more capable of isolating scanner-related noise than PCA.[63] The MNF-images exhibit a good separation of the different writing phases (figure 14): The older and younger notes and lines are visible, as well as annotations written with different inks. Overall, four main clusters were found: The new pencil lines, the new notes and the older notes. As a fourth class the older lines are co-appearing with scribbled, older annotations. These classes are shown in various combinations in the first five MNF-bands. Combined in a false-color image, MNF-Bands 1, 3 and 5 showed the best result. The younger notes appear magenta, the older notes black. Different stages of annotations are visible and discernable. As expected, the pencil lines are very brightly colored and distracting.

[63] LUO ET AL. (2016).

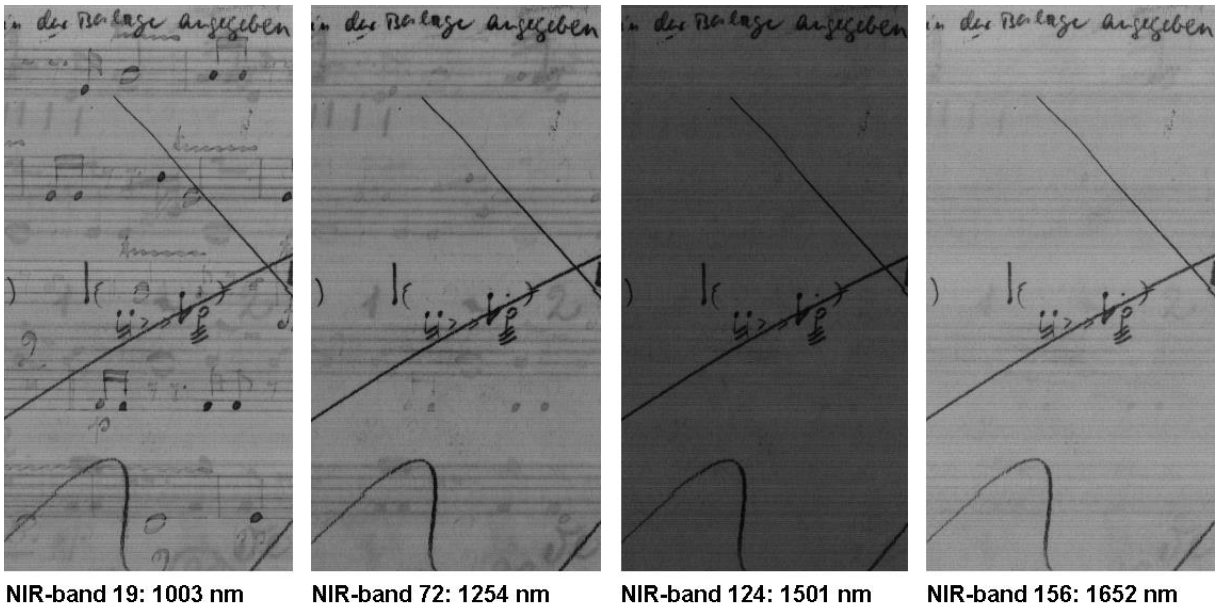

Figure 14: Four NIR-bands of the recorded cube

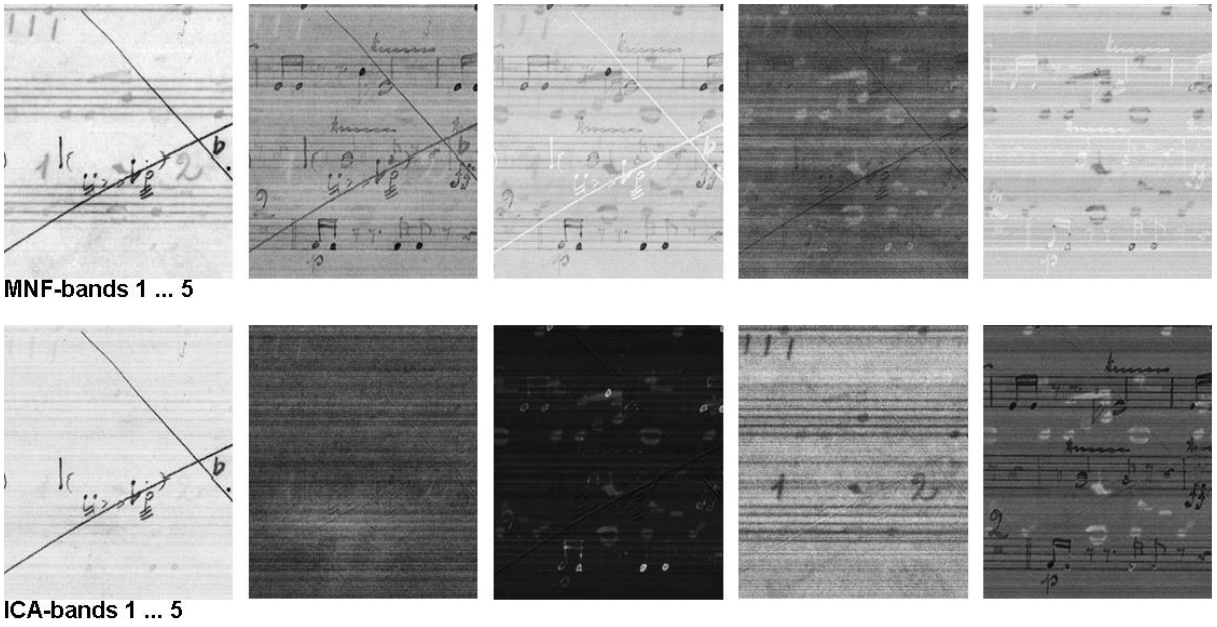

Figure 15: Comparison of MNF and ICA-bands

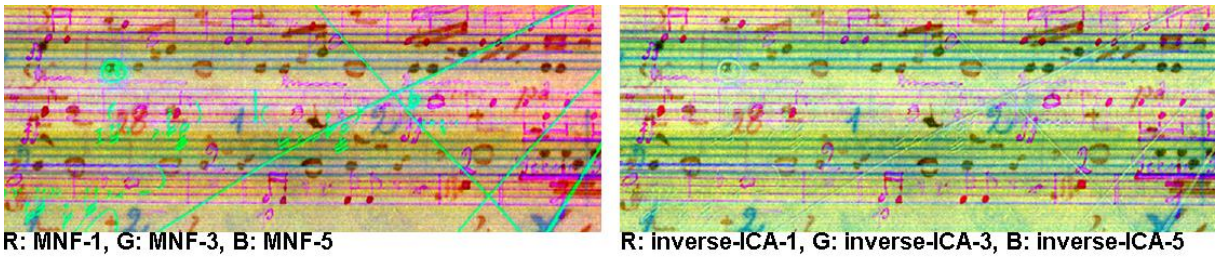

Figure 16: Composite images before (left) and after (right) the overscript removal

4.2.2.1.3 Reduction of Overwriting

To exclude the pencil-class from the composite image, a complete class-separation is necessary. MNF-5 is the only band that is almost without contribution from the pencil-class, showing a combination of older and younger inks only. Since the pencil lines are present in all other bands, they could not be excluded. A composite image from the MNF-bands showing all the necessary information therefore still comprises the disturbing lines. As the MNF-bands are uncorrelated, the addition of two bands showing opposing intensities of the pencil class (respectively: subtraction of identical intensities) could be one way to eliminate the overwriting. Since all bands show features of other classes as well, this would lead to strongly mixed bands, which would not be well suited for a composite image that should, ideally, only contain information for one of the important classes in each channel to provide distinctiveness.

To improve on this issue, the MNF-cube was transformed again using ICA on the first 20 MNF-bands. As stated earlier, ICA is a method suited for separating and isolating different components in an image, based on the assumption of their mutual independence. This is a stronger condition than uncorrelatedness for PCA and MNF, and can therefore lead to a more distinct class separation. The results in figure 15 show, that ICA was indeed able to isolate the pencil lines almost completely from the other bands, into IC-1. The other important classes (notes, lines, annotations from different phases) were not separated as well, as in the MNF. ICA is a linear transformation method and ENVI stores the transformation parameters in a statistics file. This allows for inverse-transformation, in the same way as was discussed for PCA or MNF. An inverse-transformation of the ICA was used, leaving out only the first independent component. In this way, most of the information concerning the pencil lines could be excluded, without losing relevant information on the notes. Figures 16 and 17 show the success of this method. The composite image (red: ICA-MNF band 1, green: ICA-MNF band 3, blue: ICA-MNF band 5) shows only traces of the lines, which are much less distracting than in the image using the same bands from the MNF-transform. A further improvement could be possible by spatial filtering, or selective post-processing using Photoshop, or an inpainting algorithm.

4.2.2.2 Discussion

The hyperspectral NIR-scan contained diverse information about the page. The high spectral resolution enables to discriminate, not only between the different notes, but also between annotations written with different materials, while the spatial resolution is sufficient to see small features like lines or note tails. Using linear transformation techniques it was possible to combine all relevant information and selectively exclude the distracting overwriting.

This application also shows the different functioning of MNF and ICA on this data: While both transformations basically extract the same four to five clusters and show them in different combinations, ICA performs a much stricter separation into different components than MNF. While MNF provided images at high quality, fusing the information into a few bands, ICA performed well at splitting these images into their respective independent components. The pencil-class information was concentrated completely into one component. This shows, that the class fulfills the independence-condition well, which is founded in the physical attributes of this overwriting. The pencil lines lie on top of all other classes, show a high and constant absorption across the whole spectrum and are spatially sharp and well defined. IC-2 seems to consist of systematic noise (horizontal lines) and features of the paper structure and parts of the older annotations that also show strong, continuous absorption features, similar to the pencil. Noise and paper structure are two groups, that are present across the spectral range, independent of wavelength and any other components in the data as well. In contrast to the pencil lines, these features are hardly observable in the untransformed data. This shows, that the feature extraction process is not necessarily connected to visual prominence in the original image, but can result in images, showing underlying structures in the data. The next three ICA-bands contain underlying and overlying notes, lines and annotations in different intensity-combinations. These features were separated better in the MNF. MNF, being based on PCA, transforms to extract components with high variance. The older and younger notes both show strongly and homogenously varying intensities across the cube, which explains their prominence in MNF.

Concerning this experiment of NIR-imaging selective overscript-removal, a combination of both methods, with ICA used to isolate overlying classes from a pre-transformed, uncorrelated MNF-cube, yielded good results. MNF, as a noise-corrected PCA-variant worked well on concentrating the information of interest and isolating it from the relatively high noise level.

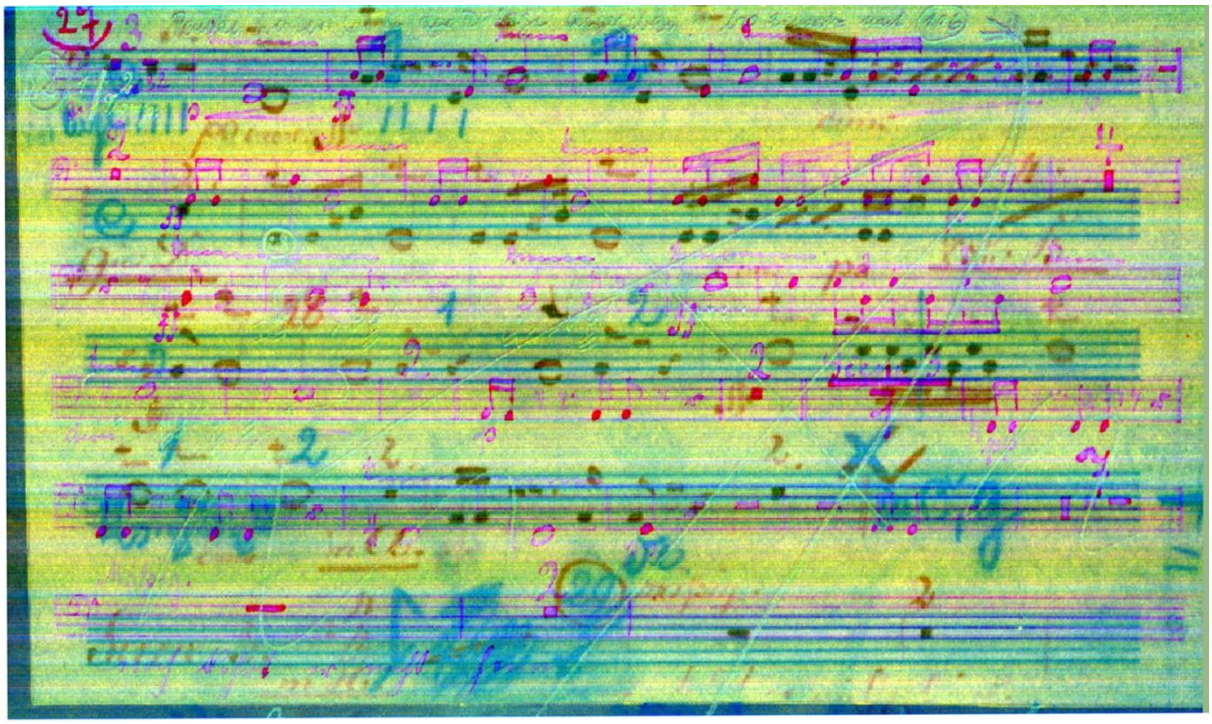

Figure 17: Transformation result (MNF-ICA: Red: Band 1, green: Band 3, Blue: Band 5. The notes and lines of the over pasted paper appear in magenta, the original notes in black. Original lines are blue, original annotations in different shades. The pencil lines were filtered out using ICA/inverse-ICA

4.2.3 Discrimination and Visualization of Different Scriptures of a Palimpsest

4.2.3.1 The "Munich Palimpsest"

The hyperspectral analysis of palimpsests will be presented using an example from the BSB: The so called "Munich Palimpsest". The manuscript shows two different scriptures: The oldest is a Hebrew text written in a brownish to reddish ink. This text will be refered to as the undertext. The second scripture, the overtext is a medieval text in Latin that has been written on top of the Hebrew text, without completely removing the older text beforehand. The text-orientation of the overscript is vertically mirrored to the underscript. The Latin text is identified as part of a copy of Paulus Orosius's *historia adversus paganos* dated to the first half of the eighth century. The Hebrew text consists of different prayers and is believed to be one of the oldest Hebrew texts, preserved in Europe.[64] Today, three fragments are attributed to the palimpsest: Two are separate pages, stored under the shelfmarks Clm 29416 and Clm 29418. The third page is still bound as paste-down in a medieval codex (Clm 6315). In Clm 29416 and Clm 6315, both scriptures show a range from well legible to almost completely faded. Clm 29416 shows a third scripture, which was presumably added rather recently and reads the shelfmark and additional annotations written with a blue-colored pencil. This writing has bled through the parchment, probably due to a past humidity damage. The separate page Clm 29418 differs strongly. The overscript is well readable and shows a variant handwriting compared to the other fragments. The underscript has been removed thoroughly, leaving only imprints of the writing visible under raking light.

The goal of this hyperspectral analysis is to evaluate, if the readability of the undertext could be enhanced using imaging techniques.

The data collected of Clm 29416 and Clm 29418 consisted of two hyperspectral image cubes of each page (VIS-NIR: 375…918 nm, and NIR: 960 nm … 1775 nm) and a digital RGB-photograph. The scans were combined, sharpened and de-noised like previously described resulting in a pre-processed image-cube with a spectral range from 400.8 nm to 1652.3 nm in 338 bands. In the following, the results on the verso of the first page are presented.

In the case of Clm 6315 the data acquisition was hindered by the book-form of the object. To prevent any damaging of the binding, the book could only be opened to 90° for the scanning process. This increased the distance between light source and object-surface from 1 cm to roughly 40 cm. At this distance, the light-source is no longer expected to provide strictly diffuse

[64] יוסף/ YAHALOM (1969).

lighting which can lead to spectral artifacts from specular reflectance. Furthermore the distance lowers the resolution of the system significantly. This object was therefore excluded from this hyperspectral analysis, but will be scanned, once an optimized illumination unit is installed.

4.2.3.2 Clm 29418

As stated before, the fragment shelfmarked as Clm 29418 is different from the other fragments attributed to the Munich Palimpsest. The underscript is barely visible in the VIS. In the NIR-region, the overscript is mostly transmissive, while the underwriting becomes visible. The clearest readability lies around 1000 nm. The application of linear transformations did not provide enhanced legibility in this case, but the NIR-images are clear enough for a first study. Compared to the other fragments, the underscript of Clm 29418 appears different. As apparent in figure 19 the characters are not Hebrew. This proves, that Clm 29418 cannot be considered part of the Munich Palimpsest. The images produced in this work will be investigated by scripture scholars in the BSB, to gain more information about this manuscript.

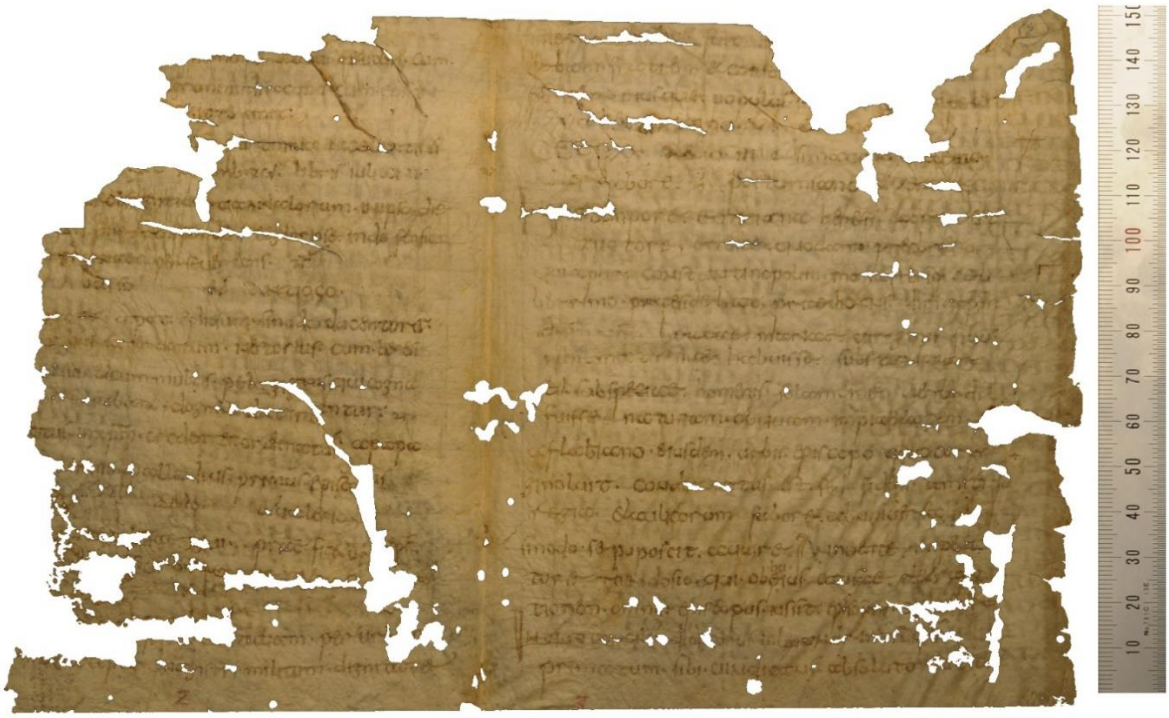

Figure 18: Clm 29418, inner side

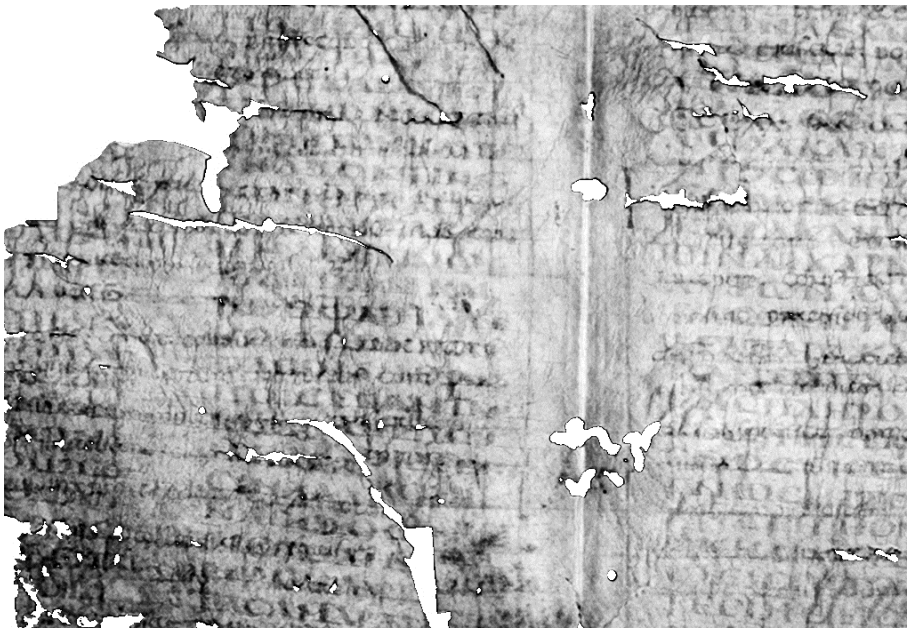

Figure 19: Subset of Clm 29418, NIR: 1051 nm. The overtext is more transmissive, leaving only the undertext visible in the NIR. The recognizable letters are not Hebrew

4.2.3.3 Clm 29416, 1-verso

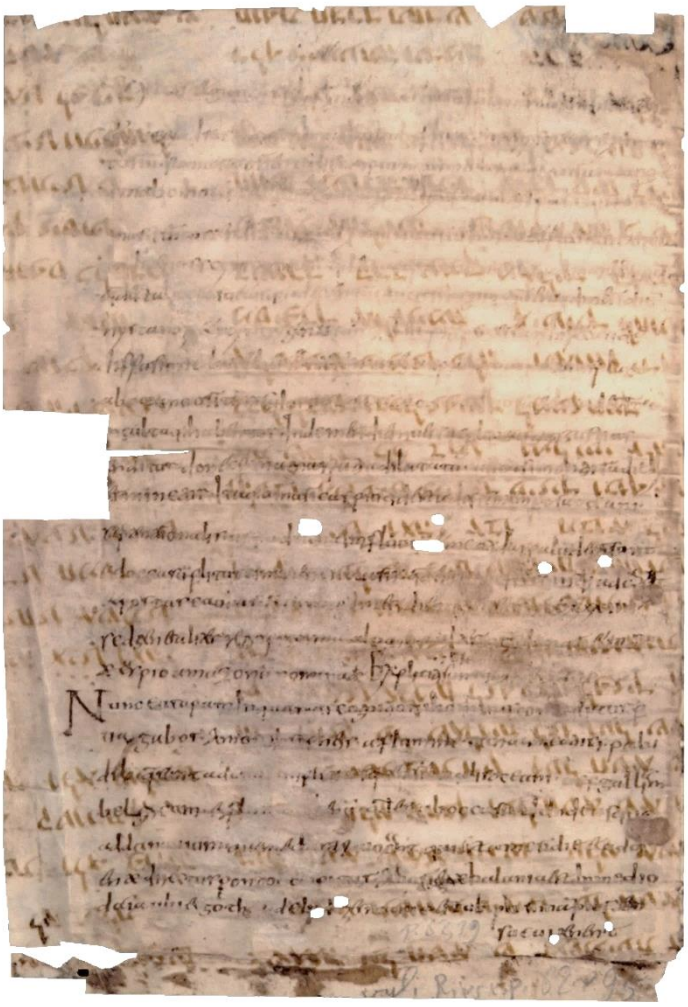

Figure 20: Clm 29416, 1-verso. RGB-composite (Red: 640.3 nm, green: 549.8 nm, blue: 470.9 nm)

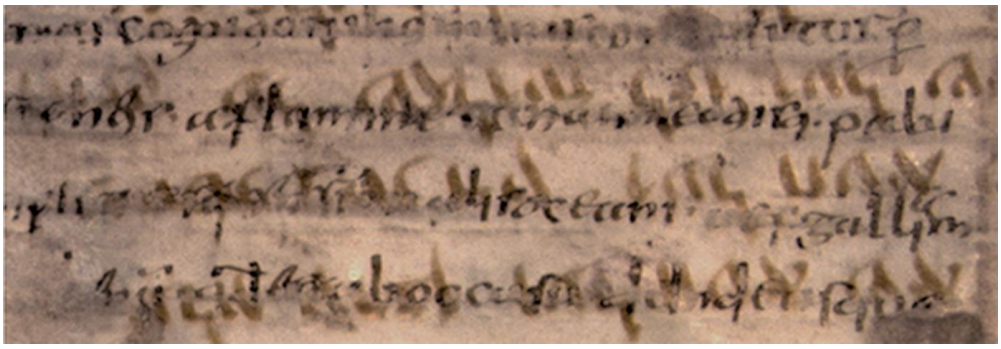

Figure 21: Subset of an area in the lower right quadrant with good visibility of both scriptures

To better understand the spectral features of the different inks, a small set of pixels was marked for each of the relevant classes (undertext, overtext, parchment) to calculate class-statistics (figure 22). These three classes and the small training areas are not sufficient to describe the whole image but approximately contain the scriptures in their best readable condition. The

class-means show similarities between the different inks, especially in the NIR-spectrum. Important differences between the scriptures lie in the VIS, where the lighter and more brownish/reddish undertext exhibits an overall stronger reflection and a steeper increase towards 800 nm, with a slight shoulder at around 600 nm. The reflection of parchment and overtext increase almost parallel, with the parchment showing a relative reflection value around 20 points higher. All classes show a minimum around 450-500 nm, but at slightly different positions. In the VIS, the overall intensity of the undertext lies between the other classes. In the NIR, the undertext shows the highest reflectivity. Apart from this, all three classes show a very similar development in the NIR. The discussed class means do not represent the classes well, considering variation across the whole page. Point spectra that were extracted on various positions of the whole page showed, that the classes are strongly varying and overlapping which renders a classification a difficult task.

In the case of the strongly faded characters (figure 23), the three classes are almost identical. The high visual and spectral similarity between the faded characters and the parchment make the classes difficult to separate by statistical methods. Nevertheless, could a decorrelation and reprojection by the afore presented transformation methods lead to a better readability, by enhancing the contrast and allowing a different “point of view” on the materials.

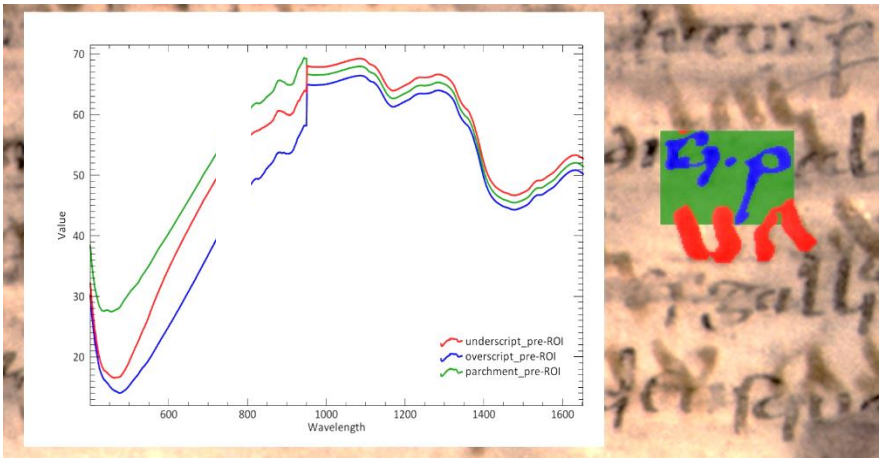

Figure 22: ROIs and their computed mean-spectra. Green: parchment, red: Underscript, blue: Overscript

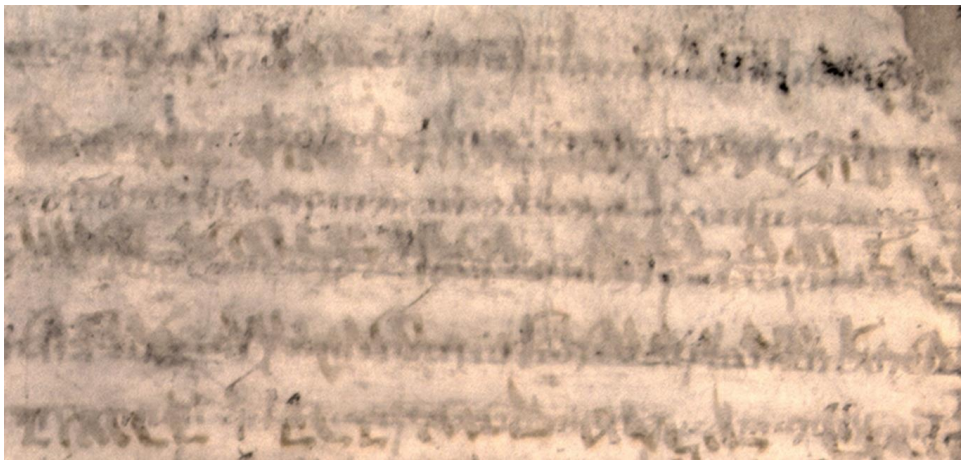

Figure 23: Clm 29416, 1-verso. RGB-composite (Red: 640.3 nm, green: 549.8 nm, blue: 470.9 nm). The subset shows an area in the upper right quadrant with strongly faded and overlying scriptures

4.2.3.4 Readability Enhancement using Unsupervised Techniques

To make the scriptures, especially the Hebrew text more legible, the unsupervised spectral transformation processes described in chapter 2 were applied. As stated earlier, the different methods are designed to extract the most unique features into the first few bands of the projected image-cube. Since the transformation methods are based on the statistics of the input image, the results greatly depend on the region, subject to the transformation. Smaller subsets often produce better results, because the variation for each class is lesser and the underlying features are easier to extract. It is therefore useful to compute the transformations multiple times on different subsets.

4.2.3.4.1 Principal Component Images

The first subset of Clm 29416 1a is shown in figure 21. The scene contains both scriptures in readable condition and a relatively homogeneous background. The image was transformed using the standardized PCA method as implemented in ENVI. The transformed components are sorted by decreasing variance. Thus, the first few bands can be assumed to contain most of the information. Figure 24 plots each component against its eigenvalue (Screeplot) to show the amount of variance captured in each component.

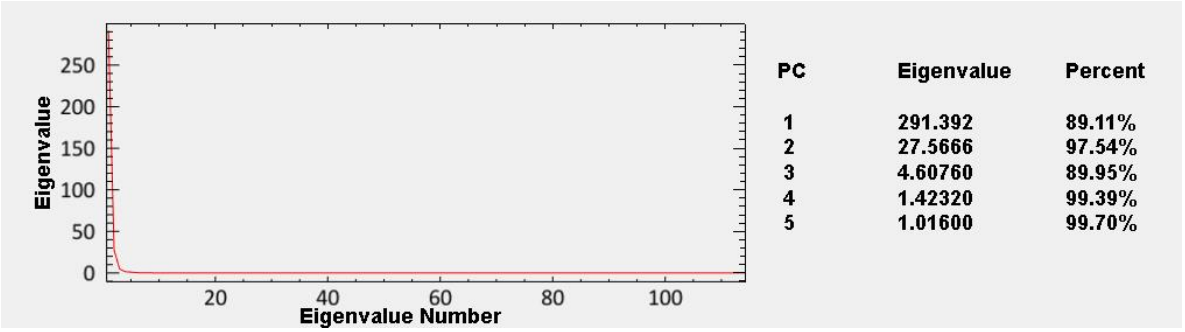

PC	Eigenvalue	Percent
1	291.392	89.11%
2	27.5666	97.54%
3	4.60760	89.95%
4	1.42320	99.39%
5	1.01600	99.70%

Figure 24: Scree-plot (left) showing the eigenvalues of the first 100 PCs and covered variance of the first 5 PCs in percent (right). Most of the variance is concentrated in the first five components

The first five PCs contain more than 99% of the images variance. PC-1 has an eigenvalue of 291, PC-5 one of 0.5. The first four PCs are shown in figure 25. Two clusters are apparent by comparing the first two PC-images. PC-1 separates the parchment from the texts by assigning high and medium intensities to the scriptures and lower intensities to the parchment. PC-2 enhances mostly the texture of the parchment. The PC-images 3 and 4 put the two scriptures in different intensity ranges but are relatively diffuse and do not provide a clear discrimination between parchment and texts. PC-3 shows glowing edges and artifacts around the letters. This is probably the result of a slight misalignment of the layers during the registration or spectral sharpening steps. The composite image of the three first components does not enhance the readability well enough. The high contrast between the colors is useful in some areas with stained or darkened parchment, but the colors are too spread out to provide a clear image. This is due to the insufficient separation of materials by the PCA, resulting in a simultaneous appearance of multiple classes in every component image.

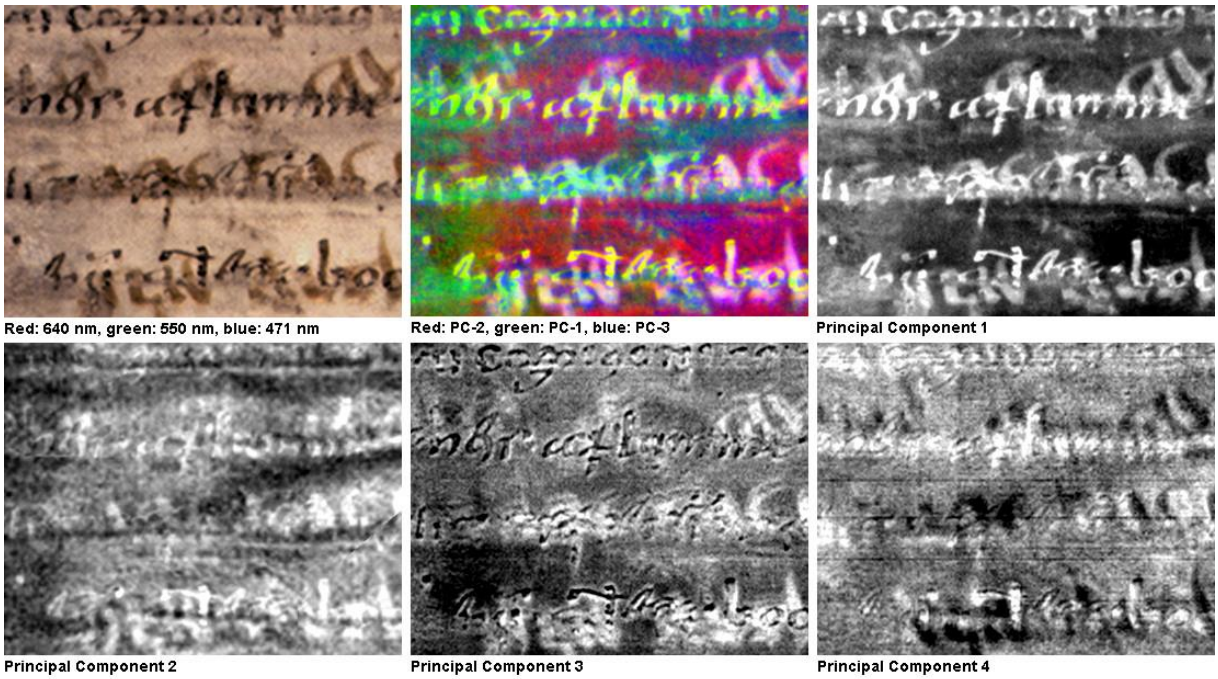

Figure 25: PC images of a subset of Clm 29416 1-verso

4.2.3.4.2 Independent Component Images

The image-cube was then transformed using ICA. Since ICA is a computational intense method, the image was pre-processed using PCA as dimensionality reduction method. ICA was then applied on a subset of the first 30 PCs with a combined variance of almost 100%. ICA was performed as implemented in ENVI. To get more precise results, the IC-threshold was set to the minimum value (0.00000001) and the iterations and stabilization iterations to 1000. The first four components are shown in figure 26.

ICA performed better in separating the classes than PCA. Each of the three classes is represented by one of the first three components with much less interference from the other classes, than in the PC-images. The information is spread over less bands than in the PCA (bands 4 to 30 show mostly noise with some darker or lighter areas, but almost no spatially coherent information). The combined image is therefore a good improvement over PCA. The overlaying characters of the two scripts in the subset could not be separated, but the high contrast facilitates the analysis of the visible parts of the obscured letters and their reconstruction. Even more than PCA, ICA was found to be dependent on the chosen subset. While whole-page PCA-transformations delivered results comparable to the small subsets, ICAs quality tended to decline with increasing subset-size. It therefore appears, that, alternatively, ICA could be applied selectively to regions that are not readable well enough in the PCA-transformation. While the ICA images perform better at separating the scriptures, they are less spatially distinct than the PCA bands. Good results were obtained by combining the very clear PC-1 with two ICA-bands to improve the separability of the scriptures (figures 27 to 29).

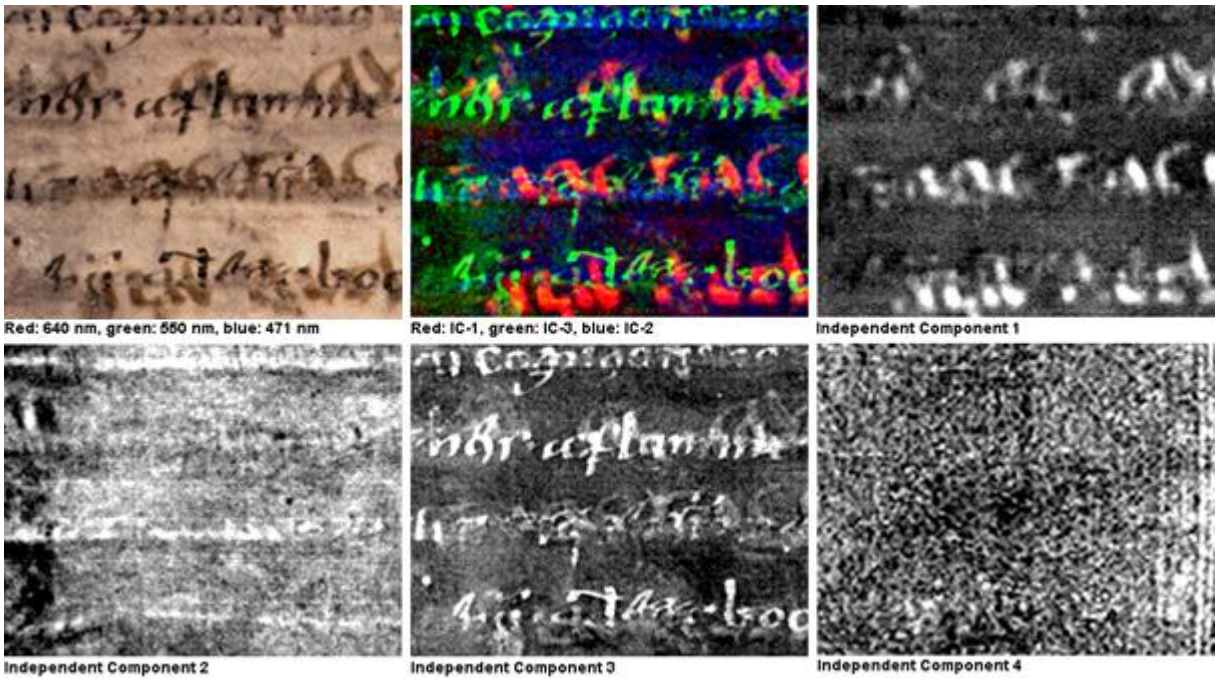

Figure 26: IC images of a subset of Clm 29416 1-verso

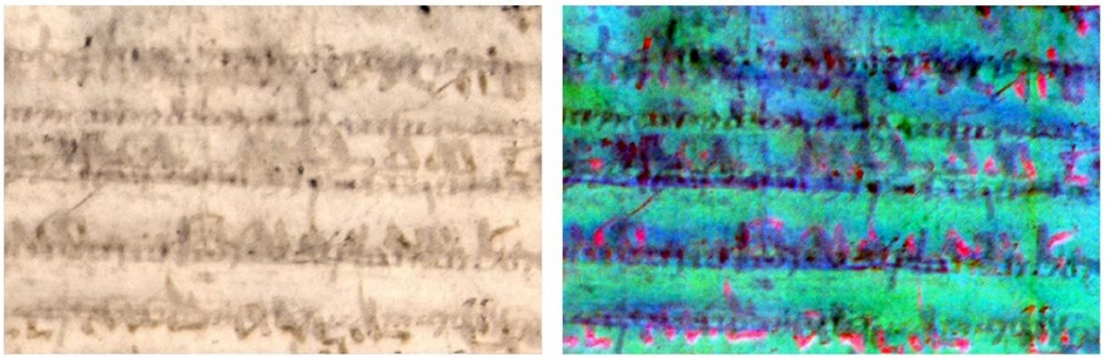

Figure 27: Clm 29416 1-verso: Composite images of a subset with faded and, overlapping characters. Left: R: 640 nm, G: 550 nm, B: 471 nm. Right: R: IC-1, G: PC-1, B: IC-4

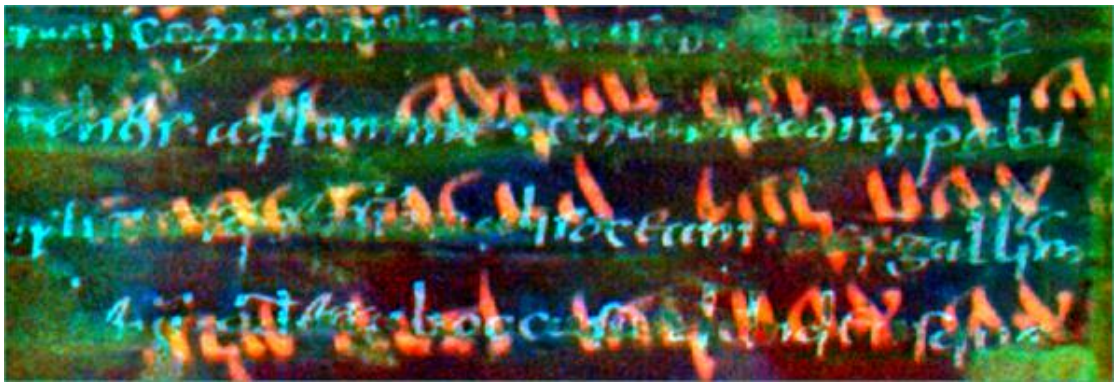

Figure 28: Clm 29416 1-verso: Composite Image of the better readable scene: Red: IC-1, green: PC-1, blue: IC-3

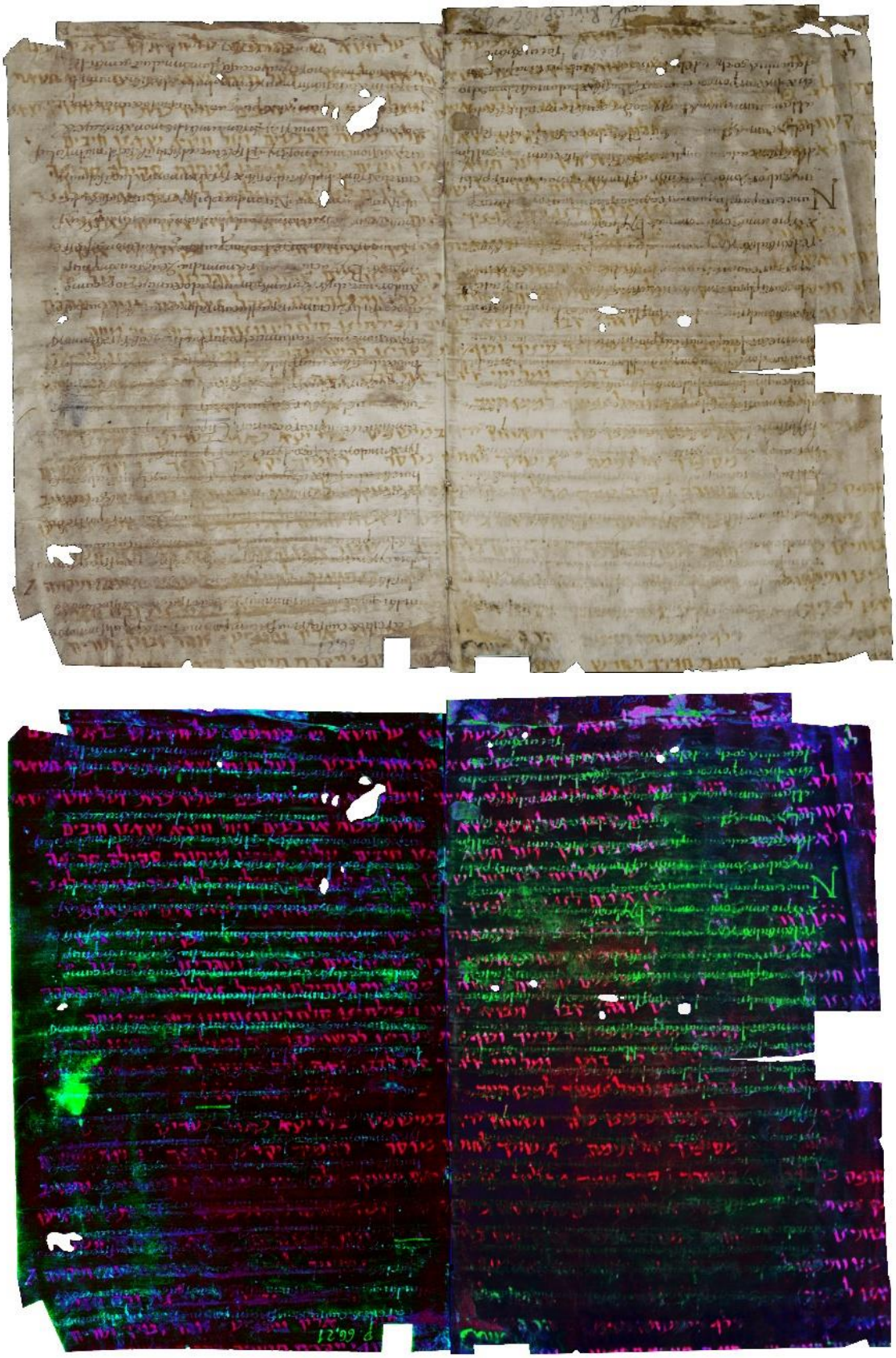

Figure 29: Cod. Clm 29416, folios 1-verso, 2-recto. Composite images: Upper Image: R: 640 nm, G: 550 nm, B: 471 nm. Lower Image: R: IC-1, G: PC-1, B: IC-4. Images were flipped by 90° to show the correct reading direction of the hebrew text

4.2.3.4.3 Discussion of Unsupervised Transformations

The analysis of the transformation results confirms, that a separation of the different writings by their spectral characteristic is possible, but strongly depending on the material under examination and the chosen methods and parameters. Especially ICA is, under beneficial conditions, able to separate the writings almost completely into two different classes. Thus, composed images with highly improved contrast between the scriptures could be produced. The best results were obtained combining a spatially sharp PCA-image with two ICA-images with superior class-separation capabilities. Yet the parts of the manuscript with worse readability remain difficult to interpret. Especially areas with overlapping and faded scriptures were not always separated well into two different bands.

This is attributed to the high variability and the similar spectral characteristics of both texts, especially in the NIR. Another problem is the spatial resolution of the NIR sensor that is not sufficient for the analysis of more detailed parts of text. In the image processing, this could be addressed by experimenting with more sophisticated image fusion tools that are less dependent on identical spectral ranges between the spatially sharp image and the image to be sharpened.[65]

To improve the discernibility, the spectral range could be extended. Most importantly a higher sensitivity in shorter wavelength regions would be useful to possibly establish more differences between the scriptures. Particularly UV-fluorescence has proven to be an important tool to differentiate inks and was used in many publications on palimpsest imaging. Since parchment usually fluoresces strongly, it also contrasts with the UV-absorbing inks.

Another possibility would be to experiment with more transformation methods. ARSENE ET AL. (2016) evaluated different methods, among which canonical variance analysis (CVA) and PCA produced the best results for readability enhancement and simultaneous visibility of both texts of a palimpsest. HOLLAUS ET AL. (2015/1) gained good results using linear discriminant analysis (LDA). Both are widely used feature selection methods that aim to increase the difference between pre-defined classes. Supervised approaches (like CVA and LDA) appear to be more successful in discriminating between very similar writings, than the unsupervised methods, presented in this work.

[65] LONCAN ET AL. (2015).

4.2.3.5 Supervised Methods

4.2.3.5.1 Supervised Classification in Readable Areas

Supervised classification has not been employed frequently In the analysis of palimpsests. To find decision rules that reliably separate letters, showing gradually changing and varying contrast to the background is not a simple task. On the other hand, the binary images produced by classification are of high value for subsequent processing, for example OCR or automated inpainting of damaged writing. Therefore, classification was applied here, to test its capabilities.

4.2.3.5.1.1 Endmember Extraction Using SMACC

To classify the images, the first step is to find suitable training data. ENVI implements a tool for automatic endmember extraction: The Sequential Maximum Angle Convex Cone (SMACC). The tool finds the most extreme vectors of a dataset, that can describe every other vector as a linear combination. These so called endmembers may not be pure materials. Unique combinations will also be registered as endmembers. Thus there are usually more SMACC-endmember than pure materials.[66] The ENVI documentation describes the working process of SMACC as follows:

"In other words, SMACC first finds the brightest pixel in the image, then it finds the pixel most different from the brightest. Then, it finds the pixel most different from the first two. The process is repeated until SMACC finds a pixel already accounted for in the group of the previously found pixels, or until it finds a specified number of endmembers. The spectra of pixels that SMACC finds become the endmembers of the resulting spectral library." [67]

While there are more sophisticated workflows of endmember extraction[68], SMACC provides a quick way to find the main underlying components in the data. SMACC was used on the subset and found 5 endmembers (figure 30).

SMACC finds only one pixel per endmember but also uses SAM to create abundance mappings, showing the probability of class-membership for each pixel and class. For supervised methods that are based on class-statistics, a pre-classification step is necessary, to expand the training data from one point, to a sufficiently large number. For this purpose, the SAM-abundance mappings created in the SMACC-workflow were thresholded to generate a classification image that shows the pixels with the highest probability to belong to a certain endmember-class. Then, a set of 1000 samples per class was selected randomly and used as training data for the classification. This delutes the high-purity endmember spectra with less

[66] GRUNINGER ET AL. (2004).
[67] http://www.harrisgeospatial.com/docs/SMACC.html
[68] DELANEY ET AL. (2010) used the ENVI spectral hourglass workflow for spectral unmixing in the imaging of a painting by Picasso.

probable finds, but generates a statistical base, that is necessary for most classifiers. All methods were also tested on smaller sample-sets, but performed better, when more training data was included. The classification was performed on the MNF-transformed dataset, to benefit from the feature extraction and noise separation capabilities of MNF.

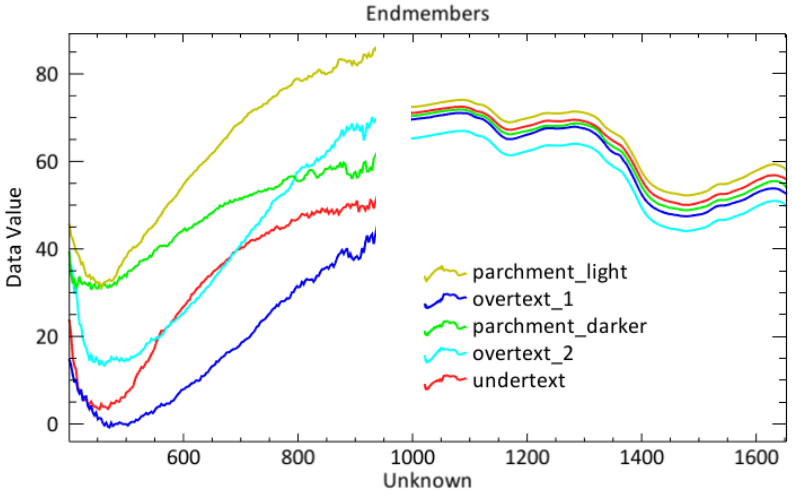

Figure 30: SMACC-endmember spectra

4.2.3.5.1.2 Classification Results

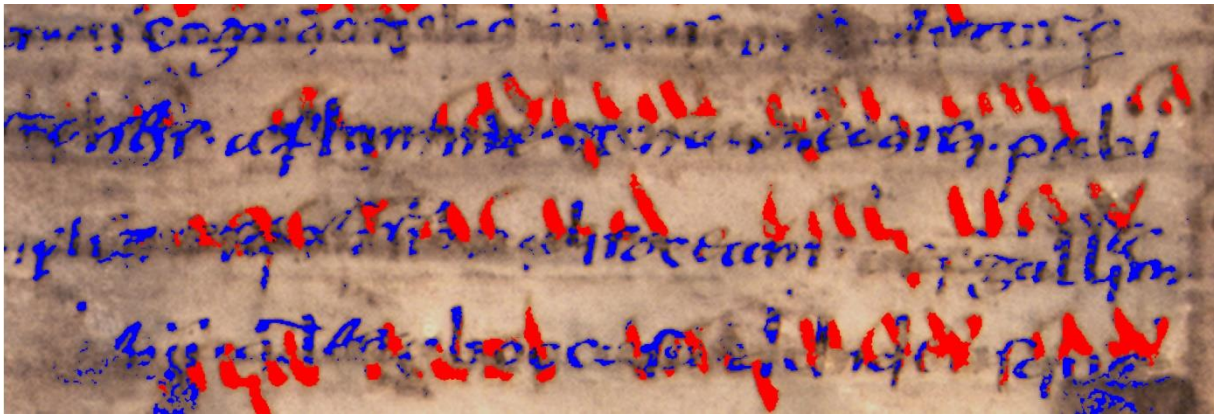

Figure 31: Clm 29416 1-verso: Classification result (Mahalanobis-distance classifier): Red: Undertext, blue: Overtext. Overlay on RGB-composite image

The following methods were tested: MinDC, MLC, MaDC and SAM. MLC and MaDC performed best on the subset. MinDC showed less scattered points, but produced more falsely classified areas. SAM was not able to map the whole subset with the provided endmembers and showed large, unclassified areas around the letters.

The classification of the subset delivered good results (figure 31). Although, the faded areas were not classified, the mappings help to visualize the scriptures which aids the interpretation.

The described process yields good results for small, consistent areas. To apply it to more difficult areas a different approach of training area definition is necessary.

4.2.3.5.2 Supervised Classification in Illegible Areas

On the more difficult subset, the above described method did not yield useful results, because of the high similarity and lack of pure, high-quality pixels for all classes in this area. Therefore a different approach was devised, using SAM as classifier/target detector. One problem of using supervised methods on the second subset was, that it was very difficult to find a sufficient number of clearly identifiable pixels for the training data. To overcome this issue HOLLAUS ET AL. (2013) adapted a line detection algorithm that automatically finds the text lines in the document image. These lines are expanded to match larger areas of the letters, to produce a binary image of the text along the text line as training data. By using the text lines as base for the training data, spatial information is taken into account to increase performance.[69]

For this present work, a more manual approach, making use of the tools in ENVI was followed. To select the text line corridors, polygonal ROIs were drawn over the areas, that an approximated majority of all characters in a text line fit into (figure 32). The remaining areas were labeled as parchment. The ROIs were not thresholded, but directly used for classification with SAM. The MNF transformed image was used, to provide the best possible discernibility for the classes. Since each ROI also contained many points from other classes, SAM was the classifier of choice, using only the spectral angle as classification criterion. In the MNF image, this angle is dominantly defined by the first few bands, in which the different scripts were visible with the best contrast to the background but too little spatial coherence to allow readability. Since the scripts account for the most variance in the respective bands, a clear discrimination between text and background, and possibly between the two scriptures should be possible, in spite of the large amount of falsely defined training points.

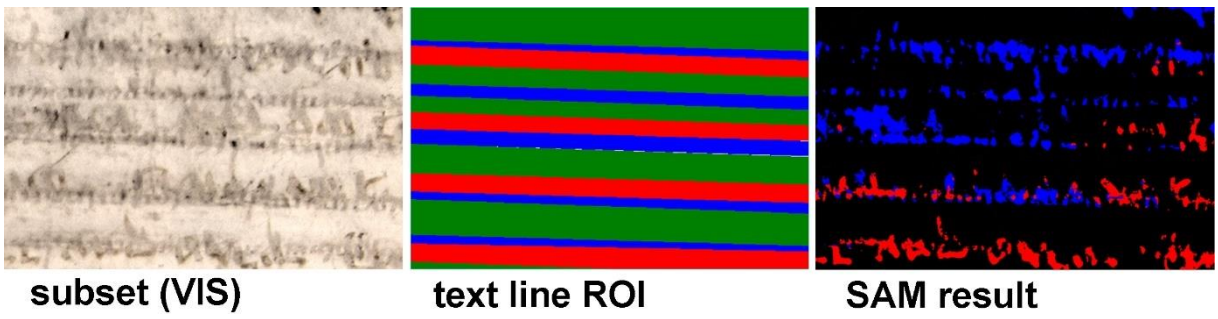

Figure 32: Left: Image of the subset. Middle: Training data selection using ROIs that mark the main areas of each text. Right: Classification results on an MNF-transformed dataset using SAM

[69] HOLLAUS ET AL. (2013), pp. 147-148.

The resulting classification image shows, that the procedure successfully combined information from different MNF-bands to classify the image. Many of the visually identifiable characters were classified correctly. On the other hand, the classification result is relatively coarse and still shows many falsely classified areas. To improve this outcome, another class was added, which was defined as the areas of intersection between the overtext lines and the undertext lines (figure 33). This class was introduced, to allow for an additional decision for text areas that SAM cannot definitively classify.

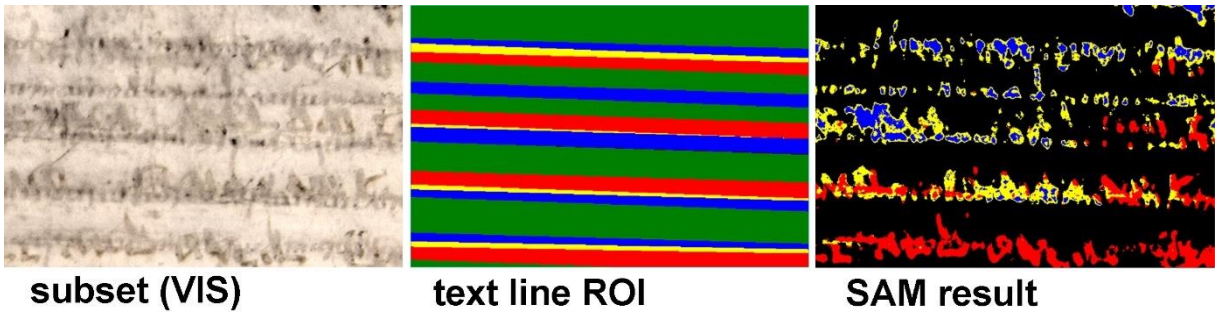

Figure 33: Middle: Addition of a new class by adding the intersections of both text ROIs. Right: Classification image (SAM, MNF-transformed data)

The classification using SAM with the text-line ROIs produced a relatively good outcome, considering the large amount of falsely-labeled training data. With the added class, the amount of false classification became lesser and more points could be classified.

4.2.3.5.2.1 Discussion of Supervised Techniques

Clm 29416 shows different levels of challenge for the classification, that are represented here by the strongly faded and the well readable subset. Several conclusions can be derived from the different performances:

The training data provided is, as expected, of high importance. To find enough training points to fulfil the requirements in untransformed hyperspectral space was not easily achievable for respective areas, considering the scarcity of points that could clearly be labeled to one of the writings. For the readable subset, a semi supervised endmember extraction workflow using SMACC, followed by a classification using MaDC or MLC was proposed, which produced good results. For the illegible subset, the developed selection method, using the text lines, provided promising results. Being quickly to apply, the method could prove to be a good first step for supervised classification or text binarization on strongly faded historic manuscripts. This could facilitate the process of supervised classification and make it more interesting for hyperspectral manuscript analysis. By refining the ROIs before classification, or experimenting with other classifiers, further improvement should be possible. With the combination of MNF-transform and SAM-classification, the approach is especially suited for hyperspectral imagery.

The classification methods tested can be considered as general-purpose classifiers. There is a variety of classification algorithms available and better results may be possible using more specialized methods. A classifier that makes use of non-linear decision rules, like ACE[70], could be helpful as well. Support vector machines (SVM) or neural networks (NN) are non-linear machine-learning algorithms that are used in many different classification tasks and could deliver an improvement.

5 Summary and Conclusion

In this thesis the importance of spectral imaging and digital image processing in the field of cultural heritage science is pointed out. Readability enhancement of palimpsests and faded historical texts in general, has proven to be a viable application of HSI. A variety of methods and algorithms can be adapted from other scientific fields, especially remote sensing. These make use of the large datasets collected with MSI/HSI, by considering mathematical, statistical and probabilistic models to filter and classify the imagery, to enhance the visibility of hidden or obscured features.

Concerning the data pre-processing it was shown, that spectral sharpening techniques can be applied to improve HSI of manuscripts. While the PC-sharpening method proposed delivered very good results, the wide field of image fusion and spectral sharpening could deliver more sophisticated methods, that could further improve the sharpening process and possibly allow for the sharpening of spectral regions outside the VIS.

In the applications, three different experiments on historical documents were presented. One application of ICA was shown on the example of the fol.1 of Msc.patr. 5 of the DNB. The enhancement of an erased text on the recto-side was hindered by artifacts from the verso side. ICAs capability as BSS-method allowed to attenuate these artifacts significantly but a weighted combination of two IC-bands proved to be most effective.

Fusion of near-infrared hyperspectral information and attenuation of distracting overtext was presented on a musical manuscript of Richard Wagner's "Götterdämmerung". Here, the relatively high level of systematic noise in the NIR imagery was successfully excluded, while the relevant information was fused into fewer bands using MNF. ICA proved to be more capable of separating the different image components and, via reverse transformation, enabled to almost completely exclude the unwanted overwritings from the image. Combining

[70] HOLLAUS ET AL. (2015/2).

the two methods provided a well readable three-band image that allows to discriminate all present writings.

In the last example, a medieval palimpsest containing a Hebrew text (Clm 29416) was examined using VIS-NIR HSI. PCA and ICA were discussed as unsupervised methods, as well as different supervised classifiers. It was found, that the result of all methods depend on the subset, suspect to the analysis. Unsupervised methods were confirmed as very capable, especially the combination of PCA and ICA combining the spatial accuracy of PCA with the stronger class-separation abilities of ICA. Supervised methods are most fruitfully performable on areas, that still show some readability. In these regions, the classifications provide easily accessible and visually appealing images, that can be used well to communicate and present the findings. Another important factor is the training data for the classifiers. While SMACC performed very well on readable areas, it was not able to deliver good training points in a more difficult region of the palimpsest. A fast and effective method, similar to the method developed by HOLLAUS ET AL. (2013) was used, to incorporate spatial information in the form of text lines into the classification process, by drawing overlapping ROIs over the spatial corridors of both scriptures, and labeling the intersections as a third class. Promising results could be produced by using these ROIs as training data for SAM on MNF-transformed data.

The presented application prove the versatility and capability of multivariate image analysis, as well on hyperspectral imagery, as on regular RGB-photographs. Especially PCA, ICA and MNF are well capable, transforming the data into various projections that provide better readability, allow for precise manipulations and can combine the information of large data-sets into few, comprehensible images. To improve the outcomes of unsupervised transformation, there is a great variety of different methods available. Dimensionality reduction methods are a core element of data mining and are becoming more and more relevant with ever growing data sets. Many of the algorithms that are published in other fields could also be applied here. A systematic study, furthering the experiments of ARSENE ET AL. (2016) could provide more algorithms that are applicable to manuscript studies.

On a further note, the presented methods also yield valuable assets for the educational mission of museums and libraries, producing appealing and intuitively understandable images, well suited for educational purposes. The images can be integrated into online presentations and catalogues to accompany the digitized manuscripts and make the scientific results available to a broader public, to raise interest and awareness of the richness of historical documents and objects in their collection.

6 List of References

ARSENE, C. T. C.; PORMANN, P. E.; AFIF, N.; CHURCH, S.; DICKINSON, M. (2016): *High performance software in multidimensional reduction methods for image processing with application to ancient manuscripts*. Retrieved 21. 01. 2018 from www.arxiv.com, arXiv:1612.06457.

CANTY, M. J. (2014): *Image Analysis, classification and change detection in remote sensing, with algorithms for ENVI/IDL and Python, third revised edition*. Boca Raton.

CHRISTENS-BARRY, W. A.; BOYDSTON, K.; FRANCE, F. G.; KNOX, T. K.; EASTON, R. L.; TOTH, M. B. (2009): *Camera system for multispectral imaging of documents*. In: BODEGOM, E.; NGUYEN, V. (eds.): *Sensors cameras and systems for industrial/scientific applications X*. Proceedings of SPIE-IS&T Electronic imaging, SPIE Vol. 7249.

DELANEY, J. K.; ZEIBEL, J. G.; THOURY, M.; … HOENIGSWALD, A. (2010): *Visible and infrared imaging spectroscopy of Picasso's Harlequin Musician: Mapping and identification of artist materials in situ*. Applied Spectroscopy, 64(6), 584-594.

DIK, J.; JANSSENS, K.; VAN DER SNICKT, G.; VAN DER LOEFF, L.; RICKERS, K.; COTTE, M. (2008): *Visualization of a lost painting by Vincent van Gogh using synchroton radiation based x-ray fluorescence elemental mapping*. Anal. Chem., 80, 6436-6442.

DORADO-MUNOZ, L.; MESSINGER, D. W.; BOVE, D. (2017): *Integrating spatial and spectral information for enhancing spatial features in the Gough map of Great Britain*. Journal of Cultural Heritage, in press, https://doi.org/10.1016/j.culher.2018.04.011.

EASTON, R. L.; KELBE, D.; CARLSON, C. F. (2014): *Statistical processing of spectral imagery to recover writings from erased or damaged manuscripts*. In: BROCKMANN, C.; FRIEDRICH, M.; HAHN, O.; NEUMANN, B.; RABIN, I. (eds.) (2014): *Proceedings of the Conference on natural sciences and technology in manuscript analysis*. University of Hamburg, centre for the study of manuscript cultures, 4-6 December, 2013. Manuscript cultures 7, Hamburg.

EASTON, R. L.; NOEL, W. (2010): *Infinite possibilities: Ten years of study of the Archimedes Palimpsest*. Proceedings of the American Philosophical Society, 154(1), 50-76.

FODOR, I. K. (2002): *A survey of dimension reduction techniques*. Technical report, Lawrence Livermore National Laboratory.
Available online at: https://e-reports-ext.llnl.gov/pdf/240921.pdf (last viewed 18.07.2018).

GELADI, P. L. M.; GRAHN, H. F.; BURGER, J. E. (2007): *Multivariate Images, Hyperspectral Imaging: Background and Equipment*. In: GELADI, P. L. M.; GRAHN, H. F. (ed.) (2007): *Techniques and applications of hyperspectral image analysis*. Chichester.

GHASSEMIAN, H. (2016): *A review of remote sensing image fusion*. Information Fusion, 32, Part A, 75-89.

GRIFFITHS, T. A. (2011): *Enhancing multispectral imagery of ancient documents.* Master-thesis, Utah State University, Department of electrical and computer engineering.

GRIFFITHS, T. A.; WARE, G. A.; MOON, T. K. (2015): *Signal processing techniques for enhancing multispectral images of ancient documents*. Presented at: *Signal processing and signal processing education workshop* (SP/SPE) 2015, Salt Lake City, UT, USA, 362-369.

GRUNINGER, J.; RATKOWSKI, A. J.; HOKE, M. L. (2004): *The sequential maximum angle convex cone (SMACC) endmember model*. In: *Algorithms and technologies for multispectral, hyperspectral and ultraspectral imagery X*, SPIE proceedings vol. 5425, Defense and security, 12-16.04.2004, Orlando, FL, USA.

HARDEBERG, J. Y.; SCHMITT, F.; BRETTEL, H. (2000): *Multispectral image capture using tunable filter*. In: ESCHBACH, R.; MARCU, G. G. (eds.) (2000): SPIE proceedings vol. 3963: Color imaging: Device-independent color, color hardcopy and graphic arts V, Electronic Imaging, 22-28.01.2000, San Jose, CA, USA.

HEDJAM, R.; CHERIET, M.; KALACSKA, M. (2014): *Constrained energy maximization and self-referencing method for invisible ink detection from multispectral historical document images*. In: ICPR 2014, 22nd international conference on pattern recognition, 24-28.08.2014, Stockholm, Sweden. Piscataway, NJ, USA, 3026-3031.

HOLLAUS, F.; GAU, M.; SABLATNIG, R. (2013): *Enhancement of multispectral images of degraded documents by employing spatial information*. In: ICDAR 2013, international conference on document analysis and recognition, 25-28.08.2013, Washington, DC, USA. Piscataway, NJ, USA, 145-149.

HOLLAUS, F.; GAU, M.; SABLATNIG, R.; CHRISTENS-BARRY, W. A.; MIKLAS, H. (2015/1): *Readability enhancement and palimpsest decipherment of historical manuscripts*. In: DUNZE, O.; SCHAßAN, T.; VOGELER, G. (ed.) (2015): *Codicology and Palaeography in the Digital Age 3*. Norderstedt, 31-46.

HOLLAUS F.; DIEM, M.; SABLATNIG, R. (2015/2): *Binarization of multispectral document images*. In: AZZOPARDI, G.; PETKOV, N.(eds.) (2015): Computer analysis of images and patterns. 16th

international conference, CAIP 2015, 02-04.09.2015, Valletta, MLT, Proceedings, Part II. Cham, Switzerland, 109-120.

IBAROLLA-ULZURRUN, E.; MARCELLO, J.; GONZALO-MARTIN, C. (2017): *Assessment of component selection strategies in hyperspectral imagery*. Entropy 2017, 19, Art. No. 666.

JAMES, A. P.; DASARATHY, B. V. (2014): *Medical Image Fusion: A survey of the state of the art*. Information Fusion, 19, 4-19.

JENSEN, J. R. (2016): *Introductory Digital Image Analysis – A remote sensing perspective*. Glenview IL, USA.

JIN ET AL. (2009) *A comparative study of target detection algorithms for hyperspectral imagery*. In: SHEN, S. S.; LEWIS, P. E. (eds.) (2009): *Algorithms and technologies for multispectral, hyperspectral and ultraspectral imagery XV*, 13-17.04.2009, Orlando, FL, USA, Proceedings of SPIE Vol. 7334, 7334W1-7334W12.

KEREKES, J. P.; SCHOTT, J. R. (2007): *Hyperspectral Imaging Systems*. In: CHANG, C. (ed.) (2007): Hyperspectral data exploiation – theory and applications. Hoboken.

KHAN, M.; CHANUSSOT, J. (2009): *Fusion of satellite images at different resolutions*. In: COLLET, C.; CHANUSSOT, J.; CHEHDI, K. (eds.) (2009): *Multivariate Image Processing*. London and Hoboken, 55-88.

LIANG, H. (2011): *Advances in multispectral and hyperspectral imaging for archaeology and art conservation*. Appl. Phys. A, 106, 309-323.

LONCAN, L.; ALMEIDA, L. B.; BIOUCAS-DIAS, J. M.; BRIOTTET, X.; CHANUSSOT, J.; DOBIGEON, N.; … YOKOYA, N. (2015): *Hyperspectral pansharpening: A review.* Retrieved 11. 01. 2018 from www.arxiv.com, arXiv:1504.04531v1.

MORISHIMA, K.; KUNO, M.; NISHIO, A.; KITAGAWA, N.; MANABE, Y.; MOTO, M.; … TAYOUBI, M. (2017): *Discovery of a big void in Khufu's Pyramid by observation of cosmic-ray muons*. Nature, 552(7685), 386-390.

NUZZILARD, D.; LAZAR, C. (2009): *Unsupervised Classification for Multivariate Images*. In: COLLET, C.; CHANUSSOT, J.; CHEHDI, K. (eds.) (2009): *Multivariate Image Processing*. London and Hoboken, 239-258.

RICHARDS, J. A., JIA, X. (2006): *Remote sensing digital image analysis*, Berlin and Heidelberg.

SALERNO, E.; TONAZZINI, A.; BEDINI, L. (2007): *Digital image analysis to enhance underwritten text in the Archimedes palimpsest*. International Journal of document analysis and recognition, 9, 79-87.

SAUNDERS/CUPITT (1993): *Image Processing at the National Gallery*: The VASARI Project. In: ASHOK, R. (ed.) (1993): National Gallery Technical Bulletin, 14, London, 72-85.

SCHNEIDER, C. A.; RASBAND, W. S.; ELICEIRI, K. W. (2012): *NIH Image to ImageJ: 25 years of image analysis.* Nature Methods, 9, 671-675.

SHLENS, J. (2014): *A Tutorial to Independent Component Analysis*. Retrieved 21.01.2018 from www.arxiv.com, arXiv:1404.2986v1.

SHRESTHA, R.; HARDEBERG, J. Y. (2013): *Multispectral imaging using LED illumination and an RGB camera*. In: Twenty-first color and imaging conference 2013 (CIC21), proceedings, 04-08.11.2013, Albuquerque, NM, USA.

SUN, W.; CHEN, B.; MESSINGER, D. W. (2014): *Nearest-neighbor diffusion-based pan-sharpening algorithm for spectral images*, Optical Engineering, 53(1), 1-11.

THURROWGOOD ET AL. (2016) *A hidden portrait by Edgar Degas*. Nature scientific reports, 6:29594.

TONAZZINI, A.; BEDINI, L.; SALERNO, E. (2004): *Independent component analysis for document restoration*. International journal of document analysis, 7(1), 17-27.

TONAZZINI, A.; SALERNO, E.; BEDINI, L. (2007): *Fast correction of bleed-through distortion in grayscale documents by a blind source separation technique*. International journal of document analysis (2007), 10(1), 17-25.

יהלום, יוסף, YAHALOM, Y. (1969): *The Munich Palimpsest and the ancient Qedushta* / פאלימפסט מינכן והקדושתה הקדומה. *Tarbiz* / לח, תרביץ, no. 1969, ד, pp. 373–383.

7 Image References

Figure 4:

Two two-dimensional, linearly mixed datasets. Image reproduced from SHLENS (2014), p. 3.

Figure 5:

The significance of training point number on class-separation. Image reproduced from RICHARDS/JIU (2006), p. 365.

Figures 9 and 10:

Images of Msc.patr. 5, fol. 1 were kindly provided by the German National Library of Bamberg.

All other images by Simon Mindermann (2018).

8 List of Imaging Hardware and Software

VNIR scanner:

Adimec A-1000 VNIR camera, manufactured by Adimec, Eindhoven, The Netherlands.

Hyperspec VNIR hyperspectral spectrometer Manufactured by Headwall Photonics, Bolton MA, USA.

NIR scanner:

Raptor Owl 320 HS NIR-camera, Manufactured by Raptor Photonics Ltd., Larne, Northern Ireland.

Hyperspec NIR hyperspectral spectrometer, Manufactured by Headwall Photonics, Bolton MA, USA.

Digital SLR-camera:

Nikon D300 S

Software:

ENVI version 5.4, Harris Geospatial Solutions Ltd., Broomfield, CO, USA.

Adobe Photoshop CS5, Adobe Systems Software Ireland Ltd., Dublin, Ireland (2014).

Image J: Available via https://imagej.net